PHYSICAL REVIEW D **88,** 075009 (2013)

Chiral-symmetric technicolor with standard model Higgs boson

Roman Pasechnik,[1,*] Vitaly Beylin,[2,†] Vladimir Kuksa,[2,‡] and Grigory Vereshkov[2,3,§]

[1]*Department of Astronomy and Theoretical Physics, Lund University, SE-223 62 Lund, Sweden*
[2]*Research Institute of Physics, Southern Federal University, 344090 Rostov-on-Don, Russian Federation*
[3]*Institute for Nuclear Research of Russian Academy of Sciences, 117312 Moscow, Russian Federation*

(Received 26 April 2013; published 22 October 2013)

Most of the traditional technicolor-based models are known to be in a strong tension with the electroweak precision tests. We show that this serious issue is naturally cured in strongly coupled sectors with chiral-symmetric vectorlike gauge interactions in the framework of the gauged linear σ model. We discuss possible phenomenological implications of such a nonstandard chiral-symmetric technicolor scenario in its simplest formulation preserving the standard model (SM) Higgs mechanism. For this purpose, we assume the existence of an extra technifermion sector confined under extra $SU(3)_{\mathrm{TC}}$ at the energy scales reachable at the LHC, $\Lambda_{\mathrm{TC}} \sim 0.1$–$1$ TeV and interacting with the SM gauge bosons in a chiral-symmetric (vectorlike) way. In the framework of this scenario, the SM Higgs vacuum expectation value acquires a natural interpretation in terms of the condensate of technifermions in confinement in the nearly conformal limit. We study the influence of the lowest-lying composite physical states, namely, technipions, technisigma, and constituent technifermions, on the Higgs sector properties in the SM and other observables at the LHC. We find that the predicted Higgs boson signal strengths in $\gamma\gamma$, vector-boson VV^*, and fermion $f\bar{f}$ decay channels can be sensitive to the new strongly coupled dynamics and are consistent with the current SM-like Higgs boson observations in the limit of relatively small Higgs-technisigma mixing. At the same time, the chiral-symmetric technicolor provides us with rich technipion phenomenology at the LHC, and its major implications are discussed in detail.

DOI: 10.1103/PhysRevD.88.075009 PACS numbers: 14.80.Ec, 14.80.Bn, 12.60.Nz, 14.80.Tt

I. INTRODUCTION

A complete experimental verification of the standard model (SM), including the discovery of the Higgs boson and precision tests of its properties, is the most intriguing and challenging task of high-energy particle physics at the moment. Last year, the major LHC collaborations, ATLAS and CMS [1,2], have announced the discovery of a new ''Higgs-like'' particle with the mass of 125.3 ± 0.6 GeV, which may become the last yet missing piece predicted within the SM framework—the Higgs boson. Some evidence for the Higgs boson has also been seen by the CDF and D0 Collaborations at the Tevatron [3].

An ultimate proof of the Higgs boson's existence and understanding of its nature would be possible only after high precision measurements of its decay parameters which can be sensitive to details of a particular new physics scenario. The current situation with the Higgs boson properties suggests that there are no significant deviations from the SM (within rather large statistical and systematical uncertainties) as revealed by the full data set collected so far at the LHC [4] and Tevatron [5] (for the most recent comprehensive studies of the Higgs boson properties, see e.g., Refs. [6–9]). Even though the room for new physics contributions has been greatly reduced [7,10], it is too early to draw final conclusions about the properties and nature of the newly discovered particle not only due to large experimental error bars, but also due to theoretical uncertainties in the SM Higgs production which are rather high and become dominant [8,11]. If the branching ratios deviate from predictions of the simplest one-doublet SM, even slightly, this would require a proper extension of the SM and pose a serious question about theoretical principles such an extension should be based upon.

Traditionally, ideas of additional-to-SM strongly coupled sectors in confinement were realized in the technicolor (TC) model, which was one of the strongest alternatives to the Higgs mechanism of the spontaneous electroweak symmetry breaking (EWSB) [12]. The existing Higgs-less TC models with dynamical EWSB (DEWSB) are based upon the idea that the Goldstone degrees of freedom (technipions) appearing after the global chiral symmetry breaking $SU(2)_L \otimes SU(2)_R \to SU(2)_W$ are absorbed by the SM weak gauge bosons which thereby gain masses. The DEWSB mechanism is then triggered by the condensate of technifermions in confinement, $\langle \tilde{Q}\,\bar{\tilde{Q}} \rangle \neq 0$. Traditional TC models with DEWSB are faced with the problem of the mass generation of standard fermions, which was consistently resolved in extended TC scenarios [13]. However, many of the existing TC models have been severely constrained or even ruled out by the EW precision data [14] (for a detailed review on the existing TC models, see e.g., Refs. [15,16]). Generally,

*Roman.Pasechnik@thep.lu.se
†vbey@rambler.ru
‡vkuksa47@mail.ru
§gveresh@gmail.com

in these schemes noticeable contributions to strongly constrained flavor changing neutral current (FCNC) processes appear together with too large contributions to Peskin-Takeuchi (especially, to S) parameters. Further developments of the TC ideas have resulted in the walking TC model, which succeeded in resolving the above-mentioned problems and remains a viable model of the DEWSB [17–19].

Very recently, as was shown in Ref. [10] based on the latest LHC data, the 1σ allowed region of the relative to SM-predicted Higgs-vector-vector fusion HVV coupling is $0.96^{+0.13}_{-0.15}$, which sets further constraints on the EWSB models alternative to the SM Higgs mechanism, as well as to composite Higgs models (see also current bounds on the rescaling of the SM couplings in Refs. [9,20]). However, even if the newly discovered particle is indeed the SM Higgs boson and the Higgs mechanism is experimentally confirmed, all available LHC and high precision EW data do not completely exclude the existence of a strongly coupled fermion sector in confinement, additional to the SM fermion sector, with a confinement scale $\sim$0.1–1 TeV being not very far from the EW scale $M_{\rm EW} \sim 100$ GeV. The main goal of this paper is to prove this statement and to study a new class of viable realistic models for an extra strongly coupled sector assisting the conventional SM Higgs mechanism at accessible energy scales, along with the study of their implications to the ongoing new physics searches at the LHC.

An alternative class of TC models usually referred to as bosonic TC scenarios include both a Higgs doublet H and a new TC sector [21–23], without referring to an origin of the Higgs doublet. The most recent realization of the bosonic TC is based upon holographic ideas [24] and allows one to explain the existence of the recently discovered Higgs-like 125 GeV particle and its possible non-standard features [25]. In this approach, strongly coupled dynamics is defined by using the AdS/CFT correspondence within the holographic approach allowing one to avoid the EW precision constraints [26–28]. In contrast to conventional (extended and walking) TC models, in bosonic TC models the mechanism of the EWSB and generation of SM fermions masses is driven by the Higgs vacuum expectation value (VEV) in the standard way, irrespectively of the (elementary or composite) nature of the Higgs field itself. Because of the linear source term in the Higgs potential, the Higgs field H develops a VEV which in turn is induced by the technifermion condensate. This means the Higgs mechanism is not the primary source of the EWSB but effectively induced by an unknown TC dynamics at high scales. For more alternatives on TC and compositeness models, see e.g., Ref. [29].

In this work, we start off with the similar ideas about the existence of an extra Higgs-like scalar field and TC nature of the SM Higgs VEV implemented in the bosonic TC models and study theoretical and phenomenological opportunities of new possible strongly coupled sectors with chiral-symmetric (vectorlike) gauge interactions. We further develop these ideas based on the gauged linear σ model [30–32] and apply it to new TC-induced degrees of freedom, in a complete analogy with low-energy hadron physics applications. In this model, which will further be referred to as the chiral-symmetric (or vectorlike) technicolor (in short, CSTC) scenario, the oblique (Peskin-Takeuchi) parameters and FCNC corrections turn out to be naturally very small and fully consistent with the current EW constraints as well as with the most recent Higgs couplings measurements at the LHC in the limit of small Higgs-technisigma mixing. Most importantly, this happens naturally in the standard quantum-field theory framework implemented in rigorous quark-meson approaches of hadron physics without attracting any extra holographic or other special arguments from unknown high-scale physics. For simplicity, we adopt the simplest version of the standard model with one Higgs doublet, and the question of whether it is elementary or composite is not critical for further considerations. The new heavy physical states of the model (additional to those in the SM) are the singlet technisigma $\tilde{\sigma}$, triplet of technipions $\tilde{\pi}_a$, $a = 1, 2, 3$, and constituent technifermions $\tilde{Q}$ which acquire masses via the technifermion condensate as an external source and the technisigma VEV (other composite degrees of freedom are usually much heavier and decoupled from the considered low-energy limit of the theory). Their possible phenomenological implications and signatures at the LHC are the subject of our analysis.

Despite the phenomenological advantages mentioned above, the proposed CSTC scenario, at least in its simplest form considered here, does not attempt to resolve the naturalness problem of the SM, i.e., does not provide a mechanism protecting the Higgs boson mass itself from becoming arbitrary large. Nevertheless, it points out a promising path towards a consistent formulation of composite Higgs models in extended chiral-gauge theories with vectorlike UV completion.[1] Indeed, the existence of composite Higgs-like bosons is often considered as a primary guideline for technicolor models. In analogy with hadron physics, composite bosons can be of two different types: *pseudo-Goldstone collective excitations*

[1]Also, the model does not provide a mechanism for generation of current (Dirac) technifermion masses which *a priori* are arbitrary. In analogy to ordinary QCD, however, we consider the physically interesting conformal limit of the new strongly coupled dynamics realized in the chiral limit of the theory $m_{U,D} \ll \Lambda_{\rm TC}$ which leads to an unambiguous determination of the Higgs VEV in terms of the technifermion condensate. The latter means that the EW symmetry is broken dynamically via the effective Higgs mechanism in this limit, which makes it particularly interesting. This statement is stable with respect to radiative corrections.

(a quantum wave of correlations between nonperturbative technifermion fluctuations in technivacuum) and *techniquarkonia* (a "bubble" of technivacuum stabilized by valence technifermions). After LHC experiments, the technicolor models with composite SM-like Higgs bosons have become favorable. The latter means that the SM-like Higgs mechanism is indeed realized in nature even though it can be treated as an effective one; i.e., the initial fields of collective excitations or techniquarkonia should be in the fundamental representation of the EW gauge group with hypercharge $Y = 1/2$. In the CSTC model, such objects naturally appear if one extends the technifermion sector. The simplest extension is such that, in addition to the EW doublet of technifermions $\tilde{Q} = (U, D)$, one introduces an extra weak-singlet technifermion S. Therefore, a new composite scalar field $\mathcal{H} = \bar{S}\tilde{Q}$ appears, having transformation properties of the Higgs boson [$SU(2)_{\rm W}$ doublet with $Y = 1/2$]. In this model, the initial classification (techniflavor) group is the global chiral group $SU_{\rm L}(3) \otimes SU_{\rm R}(3)$. A further generalization would be to consider $SU_{\rm L}(4) \otimes SU_{\rm R}(4)$ giving rise to an effective two Higgs-doublet model. Of course, in such extended techniflavor models there appear plenty of new technihadron states which require a separate lengthy analysis. In analogy to hadron physics, one may expect, however, that the lightest physical technihadron states which are the most interesting for the LHC phenomenology in the first place are technipions, technisigma, and, in principle, lightest technibaryons. Therefore, in this paper we limit ourselves to considering initially the (presumably, the *minimal*) techniflavor group $SU_{\rm L}(2) \otimes SU_{\rm R}(2)$ and discuss a simplified model with gauged vectorlike subgroup $SU(2)_{\rm L+R}$ only where the Higgs boson formally (at the low-energy part of the spectrum of technihadrons) has the status of the fundamental field, which does not satisfy the naturalness criterion. An extended techniflavor model $SU_{\rm L}(N_f) \otimes SU_{\rm R}(N_f)$ with $N_f > 2$ will be studied elsewhere.

The paper is organized as follows. Section II is devoted to a description of theoretical foundations of the CSTC scenario along with the physical Lagrangian derivation and analysis of the parameter space. The study of EW constraints (oblique corrections and FCNC) is performed in Sec. III. Some basic opportunities for LHC phenomenology, in particular, in studies of the Higgs sector properties, as well as in searches for new lightest composites, are discussed in Sec. IV. Finally, Sec. V summarizes the basic results of the paper.

II. CHIRAL-SYMMETRIC TECHNICOLOR MODEL

A. Vectorlike technifermions vs chiral SM fermions

Historically, the Nambu-Jona-Lasinio (NJL) model [33] based on the global chiral group $SU(N_f)_{\rm L} \otimes SU(N_f)_{\rm R}$ is the first model describing dynamical breaking of chiral symmetry in particles physics (for a review on the topic, see e.g., Ref. [34]). A large interest in the gauged version of the NJL model (or GNJL) initially proposed in Ref. [35] has been stimulated by its importance for constructing extended TC models and top-quark condensate models (for an extensive review of the GNJL models and their applications, see Ref. [36]). The GNJL approach has fewer parameters and significantly reduces ambiguities of corresponding predictions.

As one of the most successful implementations of the GNJL ideas in hadron physics, the so-called gauged linear σ model (GLσM), initially proposed in Ref. [30] and further elaborated in Refs. [31,32], was one of the first models with local chiral $SU(2)_{\rm R} \otimes SU(2)_{\rm L}$ symmetry, which incorporates the vector ρ and pseudovector a_1 mesons as corresponding gauge bosons, besides lightest pseudoscalar pion π and scalar σ fields. Typically, the local chiral symmetry is spontaneously broken by the scalar σ VEV giving rise to the vector-meson mass terms, constituent light quark masses [37], and the mass splitting between ρ and a_1 mesons.

In what follows, we employ the ideas of the GLσM and consider the *global* chiral $SU(N_f)_{\rm L} \otimes SU(N_f)_{\rm R}$ group in the technifermion sector $\tilde{Q}$ in the simplest case with $N_f = 2$, with its subsequent breaking (by the technisigma VEV) down to the vector subgroup $SU(2)_{\rm V\equiv L+R}$ which is then *gauged* at energy scales close to the EWSB scale. Such a "gauging," however, does not necessarily mean that one should introduce extra gauge bosons to the existing theory. The gauging procedure may also mean that corresponding fundamental technifermions interact with *already existing* gauge bosons in the SM in the low-energy effective field theory limit, which is a rather plausible opportunity we wish to explore here. In analogy with standard QCD and hadron physics, at the scale of the order of the techniconfinement scale $\Lambda_{\rm TC}$ technifermions acquire effective nonperturbative constituent masses due to the chiral symmetry breaking [37]. At lower energies the initial technifermions condense into technihadron states due to confinement. This scheme is an analogy of the chiral-invariant QHD-III model [32], where the pseudo-Goldstone technipion fields $\tilde{\pi}_a$ get the same masses (via an external source term linear in $\tilde{\sigma}$ field) and remain the physical degrees of freedom, in distinction from many other traditional TC and compositeness scenarios.

For the sake of simplicity, we consider a possible scenario of the SM extension by means of an additional chiral-symmetric (vectorlike) technifermion sector confined under the $SU(3)_{\rm TC}$ group, which is analogical to the $SU(3)_c$ color group of QCD. Such an assignment is not unique, of course, but would allow us to use direct

analogies with hadron physics.[2] The GLσM can therefore be efficiently extended to incorporate constituent technifermion-technimeson interactions as the simplest way of phenomenological description of the nonperturbative effects in technihadron dynamics at low energies. We will further refer to it below as the gauged linear technisigma model, or GLTσM. In the simplest version of this model, the nonperturbative effects are accounted for by an effective NJL-type theory of constituent technifermion interactions with the lightest technihadron states only [37]—technipions and technisigma. In the context of GLTσM we suggest the following hypothesis, which will be studied below: The energy scales of the EWSB and techniconfinement have a common quantum-topological nature and are determined by a nonperturbative dynamics of the technifermion-technigluon condensate. In particular, we would like to find specific conditions on the model parameters under which the latter hypothesis is validated. As was noted above, the technipion degrees of freedom $\tilde{\pi}_a$ are the pseudo-Goldstone fields which are usually considered as collective fluctuations of the technifermion-technigluon vacuum, while technisigma $\tilde{\sigma}$ is the lightest technigluball state—these states are not usual bound $\tilde{Q}\,\bar{\tilde{Q}}$ states and thus play a special role in the GLTσM [30–32].

From the point of view of the GLTσM, the spontaneous breaking of the *global* chiral symmetry group in the technifermion sector happens in the chiral-symmetric (vectorlike) way in complete analogy with the chiral symmetry breaking in GNJL models [32,36] as follows:

$$SU(2)_{\mathrm{L}} \otimes SU(2)_{\mathrm{R}} \to SU(2)_{\mathrm{V}\equiv\mathrm{L}+\mathrm{R}} \equiv SU(2)_{\mathrm{W}}, \qquad (2.1)$$

where the subsequent gauging of the resulting unbroken vector subgroup $SU(2)_{\mathrm{V}}$ and its identification with the weak gauge group of the SM are performed. Such gauging and identification procedures are not forbidden theoretically and lead to specific properties of the technifermion sector, which thereby make it to be very different from the chiral-nonsymmetric SM fermion sectors. It therefore means that, after the chiral symmetry breaking in the technifermion sector, the left and right components of the original Dirac technifermion fields can interact with the SM weak $SU(2)_{\mathrm{W}}$ gauge bosons with vectorlike couplings, in opposition to ordinary SM fermions, which interact under $SU(2)_{\mathrm{W}}$ by means of their left-handed components only. Note that analogous vectorlike gauge interactions are rather common and appear e.g., in the chargino sector of the minimal supersymmetric standard model.

So, in this scenario the sector of initial (current) technifermions transforms according to the local gauge $SU(2)_{\mathrm{W}} \otimes U_{\mathrm{Y}}(1)$ symmetry group and, therefore, interacts only with SM gauge bosons B, W^a, $a = 1, 2, 3$, or with $W^{\pm}$, Z^0, and γ after the SM symmetry breaking. Of course, in a complete local chiral $SU(2)_{\mathrm{L}} \otimes SU(2)_{\mathrm{R}}$ theory of technifermion-technimeson-gauge interactions, one would need to include e.g., a mixing of vector technirho $\tilde{\rho}$ with the elementary SM gauge bosons as is done in local quark-meson interaction theories [32,39] (for a review on the subject, see also Ref. [40] and references therein). However, in this work, in what follows we neglect the heavier vector and pseudovector technimesons, such that only elementary gauge B, W^a, $a = 1, 2, 3$, fields remain, and consider only the spectrum of lightest composite scalar (technisigma $\tilde{\sigma}$) and pseudoscalar (technipion $\tilde{\pi}_a$) states, relevant for the LHC measurements. Note that a reduction scheme to the left-right (LR) symmetric subgroup $SU(2)_{\mathrm{L}+\mathrm{R}}$ enables one to introduce current masses of technifermions directly into the initial Lagrangian without a need for extra fields which is considered to be advantageous. While the latter freedom may be regarded as a new form of the hierarchy problem as there must be a symmetry which protects the current up (U) and down (D) technifermion masses $m_{U,D}$ from becoming very large, we take on the phenomenological approach and consider the chiral limit of the theory with the current masses being small compared to the techniconfinement energy scale, i.e., $m_{U,D} \ll \Lambda_{\mathrm{TC}}$, in complete analogy with the chiral QCD framework. Surely, the latter issue should be addressed in a high-scale grand-unified theories-like theory which incorporates new strongly coupled fermion sectors, and this certainly goes beyond the scope of the present analysis. Additionally, chiral (axial) anomalies do not appear in this framework; it is *anomaly-safe* automatically. We will further discuss specific consequences of such new vectorlike weak interactions of the additional technifermion sector in confinement.

One should remember that identification of the local vector subgroup of the chiral group with the SM weak isospin group (2.1) is a purely phenomenological procedure which leads to correct results in the low-energy limit of the theory. In reality, of course, the global classification techniflavor group $SU_{\mathrm{L}}(2) \otimes SU_{\mathrm{R}}(2)$ has nothing to do with the EW gauge group of the SM. At the first stage, the techniflavor group is used for classification of *composite* technihadrons and, in particular, predicts the existence of technipions, technisigma, and technibaryon states. At the second stage, one notices that technifermions entering

[2]For this purpose, one could choose an extension of the gauge and fermion SM sectors motivated by a reduction from the grand-unified theories originating from e.g., the superstring-inspired $E_8 \otimes E_8'$ group with many appealing features [38]. In the latter case, one of the exceptional groups, say, E_8', can exist in confinement and, possibly, consists of a few unbroken subgroups confined at different scales, whereas the second E_8 gets broken down to the SM gauge group $G_{\mathrm{SM}} \equiv SU(3)_c \otimes SU(2)_{\mathrm{W}} \otimes U_{\mathrm{Y}}(1)$ in a straightforward way. As a realistic possibility, one of the $SU(3)$ subgroups of the original E_8' can be, in principle, identified with the TC gauge group $SU(3)_{\mathrm{TC}}$, which acts only on new additional technifermion sectors, and there are no any obstacles for it to be confined at relatively low scales being not very far from the EWSB scale (later it will be shown that the latter condition is not critical for the TC-induced EWSB).

the composite technihadrons besides technistrong interactions participate also in the fundamental EW interactions. One should therefore calculate the *EW form factors* of composite technihadrons. The corresponding EW interactions must then be also introduced at *the fundamental technifermion level* consistently with those at *the composite level technihadron level*. At the third stage, in the phenomenologically interesting low-energy limit of the theory, the EW form factors approach the renormalized EW constants (since the technihadron substructure does not emerge at relatively small momentum transfers). The latter should be calculated after *reclassification* of technihadrons under the EW group representations. This threefold generic scheme will be used below for description of EW interactions of technihadrons.

According to the standard quark-meson approaches [37,40], constituent quark loops describe nonperturbative effects at relatively small distances, whereas meson loops work at larger distances. This scheme should be realized in the CSTC model under discussion, in complete analogy with the standard quark-meson theories, and is valid up to an energy scale of typical technihadron states. Following this analogy, we consider meson (technipions $\tilde{\pi}_a$ and technisigma $\tilde{\sigma}$) interactions at the tree level and technifermion interactions (with effective constituent masses) at the one-loop level [37]. At much larger energies, one should turn into the perturbative techni-QCD framework describing technigluon and technifermion (with current masses) interactions, in analogy with the standard QCD approach.

This scenario becomes especially interesting from both the theoretical and phenomenological points of view, since it predicts the existence of the physical technimeson spectrum with relatively light pseudoscalar $\tilde{\pi}_a$ and scalar $\tilde{\sigma}$ fields.[3] The latter has quantum numbers identical to the SM Higgs boson ones. This leads to a mixing of initial $\tilde{\sigma}$ and H fields causing a possible modification of the physical Higgs boson couplings. Additionally, lightest physical technipion states $\tilde{\pi}_a$ enrich LHC phenomenology with possible new observable signatures, to be studied in detail.

B. Gauged linear technisigma model: Initial CSTC Lagrangian

As was shortly discussed in the previous section, we use the standard structure of the gauged linear σ model for low-energy TC phenomenology. Let us formulate the CSTC model in terms of the lightest composite states based on the local weak isospin symmetry group $SU(2)_{\mathrm{L+R}} = SU(2)_{\mathrm{W}}$ acting on the confined technifermion sector. The initial field content of the CSTC model in its simplest formulation is given by one LR-symmetric doublet of technifermions

$$\tilde{Q} = \begin{pmatrix} U \\ D \end{pmatrix}, \tag{2.2}$$

which forms the fundamental representation of the $SU(2)_{\mathrm{W}} \otimes U(1)_{\mathrm{Y}}$ group, the initial scalar technisigma S field which is the singlet representation, and the triplet of initial technipion fields P_a, $a = 1, 2, 3$, which is the adjoint (vector) representation of $SU(2)_{\mathrm{W}}$ [with zeroth $U(1)_{\mathrm{Y}}$ hypercharge]. Thus, in terms of the fields introduced above, the GLTσM part of the Lagrangian responsible for Yukawa-type interactions of the technifermions reads

$$\mathcal{L}_Y^{\mathrm{CSTC}} = -g_{\mathrm{TC}} \bar{\tilde{Q}} (S + i\gamma_5 \tau_a P_a) \tilde{Q}, \tag{2.3}$$

where τ_a, $a = 1, 2, 3$, are the Pauli matrices. By restricting ourselves to considering only one technifermion doublet (2.2) (the first generation), we imply that other generations, if they exist, are much heavier and split off in the mass spectrum, based on analogy with the SM, even though such an analogy is not mandatory.

In the SM, the gauge boson interactions with usual hadrons are typically introduced by means of hadronization effects [see Fig. 1(left)]. In our case, such an effect is strongly suppressed by large constituent masses of technifermions $\sim \Lambda_{\mathrm{TC}}$. Instead, the interactions of $\tilde{Q}$ and P_a fields with initial SM gauge fields B_μ and V_μ^a can be introduced via the local approximation which is illustrated in Fig. 1(right). Generally speaking, these interactions should be written in terms of nonlocal form factors since both technimesons and dressed (constituent) technifermions are the objects delocalized at energy scales exceeding the scale of nonperturbative technigluon fluctuations. We assume, however, that the latter scale is large compared to the EWSB scale and corresponding effects can be neglected at experimentally accessible energy scales. Thus, in the first approximation, one can replace the form factors by pointlike couplings as is usually done in the local quantum-field theory approach.[4] The coupling

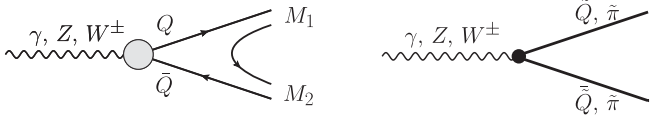

FIG. 1. An illustration of the interactions of (techni)fermion and (techni)meson fields with the SM gauge bosons via (techni)hadronization in hadron physics (left panel) and in the pointlike approximation adopted in the considered CSTC scenario (right panel).

[3]It is typically assumed that technibaryons, along with the vector and pseudovector states, are much heavier and thus likely to be irrelevant for the LHC phenomenology, at least at the moment. Although if the techniconfinement scale Λ_{TC} is not very far above the EW scale, technibaryon states might emerge in LHC data as large missing E_T signatures, which is a subject for further studies.

[4]In a more rigorous analysis this approximation can be easily lifted by introducing the Pauli form factors, although in this very first analysis of the CSTC we work in the pointlike approximation for the sake of simplicity.

constants of $\tilde{Q}$ and P_a with gauge fields can be taken the same as in the SM but calculated via the renormalization group evolution at corresponding scales. Since this evolution is logarithmic and rather weak, whereas $\Lambda_{\rm TC}$ is assumed to be in the vicinity of the EW scale, in the leading-order numerical analysis below we fix all the relevant couplings at the M_Z scale.

The vectorlike gauge interactions can be introduced via covariant derivatives over the local $SU(2)_{\rm W} \otimes U(1)_{\rm Y}$ group in the same form as the SM gauge interactions; i.e., the additional (to the SM) kinetic terms have the following form:

$$\mathcal{L}^{\rm CSTC}_{\rm kin} = \frac{1}{2}\partial_\mu S \partial^\mu S + \frac{1}{2} D_\mu P_a D^\mu P_a + i\bar{\tilde{Q}}\,\hat{D}\,\tilde{Q}, \quad (2.4)$$

where the covariant derivatives of the $\tilde{Q}$ and P_a fields read

$$\begin{aligned} \hat{D}\,\tilde{Q} &= \gamma^\mu\left(\partial_\mu - \frac{iY_{\tilde{Q}}}{2} g' B_\mu - \frac{i}{2} g W^a_\mu \tau_a\right)\tilde{Q}, \\ D_\mu P_a &= \partial_\mu P_a + g\epsilon_{abc} W^b_\mu P_c, \end{aligned} \quad (2.5)$$

respectively. Furthermore, we wish to employ analogies with the SM and, in particular, with QCD as much as possible, so for the sake of convenience and simplicity in actual calculations we fix the hypercharge of the technifermion doublet (2.2) to be the same as that of the quark doublet in the SM, i.e., $Y_{\tilde{Q}} = 1/3$, unless noted otherwise. Certainly, the hypercharge $Y_{\tilde{Q}}$, the number of technifermion generations, the respective properties of interactions, etc., should be ultimately constrained in extended chiral-gauge or grand-unified theories incorporating extra technifermion sectors, which is a subject of further studies.

In Eqs. (2.4) and (2.5), we notice two key differences of the CSTC scenario from traditional TC-based models (cf. Refs. [14,29])—the existence of physical technisigma and technipion states, introduced via the GLTσM approach, and the equivalence of left and right technifermion chiralities in their interactions with weak gauge bosons, following from the gauging of the initial chiral group of the linear σ model. Along with the absence of chiral anomalies, the CSTC scenario under discussion can be considered as a solid theoretically motivated basis for a whole new class of more elaborate TC-based extensions of the SM and their phenomenological tests.

Next, let us consider the potential part of the CSTC model Lagrangian giving rise to (pseudo)scalar self-interactions and $\tilde{\pi}$ and $\tilde{\sigma}$ masses after the chiral symmetry breaking and the EWSB. As was mentioned in the introduction, in the simplest formulation of the CSTC model developed in this work we keep the SM Higgs mechanism of the EWSB and the one-Higgs-doublet SM untouched and simply add extra technifermion sector (2.2) in confinement. As an essential part of the CSTC model, we introduce the interaction terms between the standard Higgs doublet $\mathcal{H}$ and the new P_a and S states which are allowed by the local $SU(2)_W$ symmetry. As will be demonstrated below, such extra terms lead to a mixing between the scalar Higgs and technisigma fields. The most general form of the Lagrangian corresponding to the scalar self-interactions including μ terms is as follows [40]:

$$\begin{aligned} \mathcal{L}^{\rm CSTC}_{U,\rm self} = {} & \frac{1}{2}\mu_{\rm S}^2(S^2 + P^2) + \mu_{\rm H}^2\mathcal{H}^2 - \frac{1}{4}\lambda_{\rm TC}(S^2 + P^2)^2 \\ & - \lambda_{\rm H}\mathcal{H}^4 + \lambda\mathcal{H}^2(S^2 + P^2), \end{aligned} \quad (2.6)$$

and the extra linear "source" term appears after averaging over the technifermion vacuum fluctuations and describes interactions of the scalar singlet S field with scalar modes of the technifermion condensate, i.e.,

$$\mathcal{L}^{\rm CSTC}_{U,\rm source} = -g_{\rm TC} S\langle\bar{\tilde{Q}}\,\tilde{Q}\rangle. \quad (2.7)$$

The potential part of the GLTσM Lagrangian is then given by

$$\mathcal{L}^{\rm CSTC}_{U} = \mathcal{L}^{\rm CSTC}_{U,\rm self} + \mathcal{L}^{\rm CSTC}_{U,\rm source}. \quad (2.8)$$

In Eq. (2.6), we defined $P^2 \equiv \sum_a P_a P_a = \tilde{\pi}^0\tilde{\pi}^0 + 2\tilde{\pi}^+\tilde{\pi}^-$, whereas gauge-Higgs interaction terms are the same as in the SM.

The mixing between the Higgs boson and scalar technisigma fields is governed by the quartic Higgs-TC coupling λ in Eq. (2.6). Such a mixing is one of the characteristic effects of the chiral-symmetric technicolor. In a sense, this effect is indeed one of the motivations of the model under discussion. It has to be taken into consideration if the precision LHC measurements uncover possibly small deviations of the Higgs-like 126 GeV boson (especially, in the $\gamma\gamma$ decay channel) from the standard Higgs boson. The quartic coupling λ controls such a mixing and *a priori* is allowed by the gauge symmetry of the initial Lagrangian and, thus, cannot be identically equal to zero. Indeed, any terms which are allowable by the initial symmetry of the model, even being equal to zero at the tree level, necessarily appear in divergent radiative corrections. In order to renormalize such divergencies, one has to introduce corresponding counterterms. So if at a given scale μ_0 the coupling $\lambda(\mu_0) \to 0$ vanishes, it will reappear at another scale. In particular, before the spontaneous EW symmetry breaking, the operator $\sim\mathcal{H}^2(S^2 + P^2)$ is supported by the two-loop box-box diagram illustrated in Fig. 2(left) with incoming initial S and P_a fields and outgoing initial Higgs field $\mathcal{H}$. This operator thus contributes to renormalization of λ coupling. After the EWSB, the resulting physical $h\tilde{\sigma}$ mixing is renormalized by the two-loop triangle-triangle diagram shown in Fig. 2(right).[5] In extended $SU_{\rm L}(N_f) \otimes SU_{\rm R}(N_f)$ models mentioned above,

[5]In addition, there is an extra one-loop contribution to the $h\tilde{\sigma}$ mixing which is going via a technipion loop. The latter correction exists for nonzeroth tree-level $\lambda_{\rm tree} \neq 0$ only.

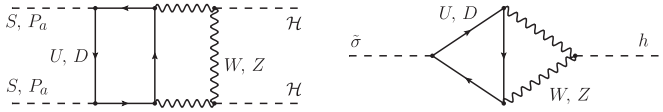

FIG. 2. Typical radiative corrections to the quartic Higgs-TC coupling λ (in particular, giving rise to the $h\tilde{\sigma}$ mixing) before the EWSB (left) and after the EWSB (right).

the corresponding quartic Higgs-TC operator which mixes physical h and $\tilde{\sigma}$ appears automatically from the main invariant of the linear σ model and cannot be eliminated.

In order to provide the EWSB and the chiral symmetry breaking in the simplest way, the Higgs $\mathcal{H}$ and technisigma S fields get VEVs and corresponding physical scalar degrees of freedom are mixed up, i.e.,

$$\begin{aligned} \mathcal{H} &= \frac{1}{\sqrt{2}}\begin{pmatrix} \sqrt{2}i\phi^- \\ H + i\phi^0 \end{pmatrix}, \qquad H = v + hc_\theta - \tilde{\sigma}s_\theta, \\ \langle \mathcal{H} \rangle &= \frac{1}{\sqrt{2}}\begin{pmatrix} 0 \\ v \end{pmatrix}, \qquad v = \frac{2M_W}{g} \simeq 246 \text{ GeV}, \\ S &= u + hs_\theta + \tilde{\sigma}c_\theta, \qquad \langle S \rangle = u \gtrsim v, \end{aligned} \tag{2.9}$$

where M_W is the W boson mass; v and u are the Higgs boson and technisigma $\tilde{\sigma}$ VEVs, respectively; h and $\tilde{\sigma}$ are the corresponding physical fields with positively definite masses M_h and $M_{\tilde{\sigma}}$, respectively; $c_\theta \equiv \cos\theta$, $s_\theta \equiv \sin\theta$, and θ is the mixing angle, which diagonalizes the respective scalar mass form. We therefore end up with the physical Lagrangian which describes new types of interactions, namely, between Higgs boson, technipions, and technisigma, Yukawa technifermion interactions, as well as mixing effects between the Higgs boson and technisigma fields, relevant for the LHC phenomenology.

As is well known, in the SM framework we deal with two energy scales of a completely different nature. The first one is the scale of the quark-gluon condensate which has a quantum-topological nature. The second one given by the amplitude of the constant Higgs field (VEV) has a classical (nonquantum) origin. In the framework of the CSTC model, we suggest another *interpretation* of the classical Higgs mechanism in which the nature of all energy scales (including the Higgs VEV) is quantum topological, in the essence of original TC and compositeness models of the DEWSB. The simplest way to realize this idea is to introduce into the scalar potential an "external source" term [the first term in Lagrangian (2.8) linear in the S field] which describes interactions between the technifermion condensate and the singlet scalar S field [40]. As will be demonstrated below, in the framework of the CSTC model this term leads to a close connection between the Higgs and technifermion condensates. A possible experimental verification of the CSTC model at the LHC relies on our assumption that both the EW and TC scales are relatively close to each other, within the LHC energy scales. Indeed, in this case it is natural to assume that the Higgs and technifermion condensates (v and u, respectively) may have the same origin. Our specific goal is to study possible observable effects of such a phenomenon related, in particular, to the Higgs boson properties as well as to lightest technihadron phenomenology at the LHC energy scales.

C. Parameter space of the CSTC model

As was mentioned above, in the framework of the CSTC scenario it is assumed that the EWSB in the SM sector (via the ordinary Higgs mechanism by the Higgs VEV v) and the chiral symmetry breaking in the TC sector (via the scalar technisigma field VEV u) may happen at energy scales relatively close to each other, i.e., $u \sim \Lambda_{\rm TC} \sim 0.1$–$1$ TeV. In what follows, we adopt this limiting case where one may expect possible specific signatures of the chiral-symmetric strongly coupled sectors potentially observable at the LHC.

Minimizing the potential (2.8) by using expressions (2.9), one arrives at the set of tadpole equations for the vacuum expectation values:

$$\begin{aligned} \langle \delta \mathcal{L}_U^{\rm CSTC}/\delta \mathcal{H} \rangle &= v(\mu_{\rm H}^2 - \lambda_{\rm H} v^2 + \lambda u^2) = 0, \\ \langle \delta \mathcal{L}_U^{\rm CSTC}/\delta S \rangle &= u\left(\mu_{\rm S}^2 - \frac{g_{\rm TC}\langle \bar{Q}Q \rangle}{u} - \lambda_{\rm TC} u^2 + \lambda v^2\right) = 0. \end{aligned} \tag{2.10}$$

The solution of the above equations with respect to scalar fields VEVs has the following form:

$$v^2 = \frac{\lambda_{\rm TC}\mu_{\rm H}^2 + \lambda(\mu_{\rm S}^2 + m_{\tilde{\pi}}^2)}{\lambda_{\rm TC}\lambda_{\rm H} - \lambda^2}, \qquad u^2 = \frac{\lambda_{\rm H}(\mu_{\rm S}^2 + m_{\tilde{\pi}}^2) + \lambda\mu_{\rm H}^2}{\lambda_{\rm TC}\lambda_{\rm H} - \lambda^2}, \tag{2.11}$$

where

$$m_{\tilde{\pi}}^2 = -\frac{g_{\rm TC}\langle \bar{\tilde{Q}}\,\tilde{Q} \rangle}{u}, \qquad \langle \bar{\tilde{Q}}\,\tilde{Q} \rangle < 0, \qquad g_{\rm TC} > 0 \tag{2.12}$$

is the technipion mass squared proportional to the (negative-valued) technifermion condensate $\langle \bar{\tilde{Q}}\,\tilde{Q} \rangle$, similarly to that in low-energy hadron physics. The vacuum stability is ensured by the minimum of the potential $U = -\mathcal{L}_U^{\rm CSTC}$ (2.8), i.e., by

$$\begin{aligned} \Delta \equiv \left\langle \frac{\delta^2 \mathcal{L}_U^{\rm CSTC}}{\delta\mathcal{H}\delta S} \right\rangle^2 - \left\langle \frac{\delta^2 \mathcal{L}_U^{\rm CSTC}}{\delta\mathcal{H}^2} \right\rangle \left\langle \frac{\delta^2 \mathcal{L}_U^{\rm CSTC}}{\delta S^2} \right\rangle < 0, \\ \left\langle \frac{\delta^2 \mathcal{L}_U^{\rm CSTC}}{\delta\mathcal{H}^2} \right\rangle < 0, \qquad \left\langle \frac{\delta^2 \mathcal{L}_U^{\rm CSTC}}{\delta S^2} \right\rangle < 0, \end{aligned}$$

leading to

$$\lambda_{\rm TC} > -\frac{m_{\tilde{\pi}}^2}{2u^2}, \qquad \lambda_H > 0, \tag{2.13}$$

which are automatically satisfied for the positively defined scalar mass form, i.e., for $M^2_{\tilde{\sigma}} > 0$ and $M^2_h > 0$.

Notice that in the limiting case of $\mu_{\mathrm{S,H}} \ll m_{\tilde{\pi}}$ which, in principle, is not forbidden (while the origin of μ terms is generally unclear in the SM theory) and even can be motivated in the nearly conformal limit of new strongly coupled dynamics (see below), both VEVs v and u are expressed in terms of the technifermion condensate, having thereby the same dynamical origin. The extra confined TC sector is now responsible for the EWSB in the CSTC model, so the role of extra μ terms, which are usually required for the classical Higgs mechanism in the rigorous SM formulation, is taken over by the technifermion condensate. This observation thus supports the above argument about the common quantum-topological nature of the EWSB and the chiral symmetry breaking mechanisms in the considering CSTC model. In what follows, we discuss both cases. In the first case, for the sake of generality, we keep the scalar μ terms permitted by the gauge symmetry as free independent parameters. In the second theoretically motivated limiting case $\mu_{\mathrm{S,H}} \ll m_{\tilde{\pi}}$, we will also consider the minimal CSTC model neglecting the small μ terms below.

In the general case, the mass form of the scalar fields can be diagonalized and represented in the form

$$\Delta\mathcal{L}^{\mathrm{CSTC}}_{\mathrm{sc}} = -\tfrac{1}{2}[m^2_{\tilde{\pi}}(2\tilde{\pi}^+\tilde{\pi}^- + \tilde{\pi}^0\tilde{\pi}^0) + M^2_{\tilde{\sigma}}\tilde{\sigma}^2 + M^2_h h^2], \tag{2.14}$$

where the technipion mass squared expressed in terms of VEVs and scalar self-couplings is

$$m^2_{\tilde{\pi}} = \lambda_{\mathrm{TC}}u^2 - \lambda v^2 - \mu^2_{\mathrm{S}}, \tag{2.15}$$

and the technisigma and Higgs boson masses squared are

$$\begin{aligned} M^2_h &= \frac{1}{2}\Big[2\lambda_{\mathrm{TC}}u^2 + m^2_{\tilde{\pi}} + 2\lambda_{\mathrm{H}}v^2 \\ &\quad - \sqrt{(2\lambda_{\mathrm{TC}}u^2 + m^2_{\tilde{\pi}} - 2\lambda_{\mathrm{H}}v^2)^2 + 16\lambda^2u^2v^2}\Big], \\ M^2_{\tilde{\sigma}} &= \frac{1}{2}\Big[2\lambda_{\mathrm{TC}}u^2 + m^2_{\tilde{\pi}} + 2\lambda_{\mathrm{H}}v^2 \\ &\quad + \sqrt{(2\lambda_{\mathrm{TC}}u^2 + m^2_{\tilde{\pi}} - 2\lambda_{\mathrm{H}}v^2)^2 + 16\lambda^2u^2v^2}\Big], \end{aligned} \tag{2.16}$$

respectively. Finally, the expression for the $h\tilde{\sigma}$-mixing angle reads

$$\tan 2\theta = \frac{4\lambda uv}{2\lambda_{\mathrm{TC}}u^2 + m^2_{\tilde{\pi}} - 2\lambda_{\mathrm{H}}v^2}, \tag{2.17}$$

whereas the sign of s_θ is given by

$$\mathrm{sgn}(s_\theta) = \mathrm{sgn}\left(\frac{\lambda uv}{2\lambda_{\mathrm{H}}v^2 - M^2_h}\right). \tag{2.18}$$

In general, the additional sector of the Lagrangian under discussion together with the modified SM Higgs sector contains seven parameters in total, namely,

$$\mu^2_{\mathrm{H}}, \quad \mu^2_{\mathrm{S}}, \quad \lambda_{\mathrm{H}}, \quad \lambda_{\mathrm{TC}}, \quad \lambda, \quad g_{\mathrm{TC}}, \quad \langle\bar{\tilde{Q}}\,\tilde{Q}\rangle. \tag{2.19}$$

In phenomenological studies, it can be convenient to turn to a mathematically equivalent set of other independent physical parameters, namely,

$$M_h, \quad M_{\tilde{\sigma}}, \quad m_{\tilde{\pi}}, \quad M_W, \quad M_{\tilde{Q}}, \quad g_{\mathrm{TC}}, \quad s_\theta, \tag{2.20}$$

where $M_{\tilde{Q}} = g_{\mathrm{TC}}u$ is the constituent technifermion mass. For this purpose, the following relations between scalar self-couplings and physical quantities (2.20) following directly from Eqs. (2.15), (2.16), and (2.17) can be useful:

$$\begin{aligned} 2\lambda_{\mathrm{TC}}u^2 &= -m^2_{\tilde{\pi}} + M^2_{\tilde{\sigma}}c^2_\theta + M^2_h s^2_\theta, \\ 2\lambda_{\mathrm{H}}v^2 &= M^2_{\tilde{\sigma}}s^2_\theta + M^2_h c^2_\theta, \\ 2\lambda uv &= \pm(M^2_{\tilde{\sigma}} - M^2_h)c_\theta s_\theta. \end{aligned} \tag{2.21}$$

In reality, two mass parameters in Eq. (2.20) can be fixed by the SM phenomenology, namely, $M_W \simeq 80.4$ GeV and $M_h \simeq 125.3$ GeV, so effectively only five-dimensional parameter space remains to be analyzed. Apparently, two phenomenologically interesting cases are possible: The lightest observed scalar particle is indeed the Higgs boson and then $M_h < M_{\tilde{\sigma}}$, or the technisigma is the lightest one and $M_{\tilde{\sigma}} < M_h$. In Eq. (2.21), we restrict ourselves to the first solution for λ, with a "plus" sign, and fix $\cos\theta > 0$ such that the sign of λ is the same as the sign of s_θ for $M_{\tilde{\sigma}} > M_h$, opposite to the sign of s_θ for reversed hierarchy $M_{\tilde{\sigma}} < M_h$. In what follows, we work with the direct mass hierarchy with the lightest Higgs boson in the scalar sector of the model $M_{\tilde{\sigma}} > M_h$, unless noted otherwise.

In Fig. 3, we represent the dependence of the quartic TC self-coupling λ_{TC} on the $h\tilde{\sigma}$-mixing angle, or more precisely s_θ, over reasonable ranges of g_{TC}, $M_{\tilde{Q}}$, $m_{\tilde{\pi}}$, and $M_{\tilde{\sigma}}$ parameters. One notices that λ_{TC} vanishes in the maximal $h\tilde{\sigma}$-mixing limit $s_\theta \to 1$ for any g_{TC}, $M_{\tilde{Q}}$, and $M_{\tilde{\sigma}}$ values and for small $m_{\tilde{\pi}} \sim 150$ GeV. For small mixing angles and rather large $M_{\tilde{\sigma}} \gtrsim 700$ GeV and $g_{\mathrm{TC}} \gtrsim 8$, it can become very large $\lambda_{\mathrm{TC}} \sim 100$, where the nonlinear nonperturbative effects turn out to be important, and applicability of the corresponding GLTσM may be restricted. This has to be taken into consideration in analysis of the available parameter space of the model and possible phenomenological signatures.

Similarly, the quartic Higgs-TC coupling λ and the quartic Higgs boson self-coupling λ_{H} with respect to s_θ are given in Figs. 4 and 5, respectively. The λ coupling does not depend on the technipion mass and vanishes in both limits $s_\theta \to 1$ and $s_\theta \to 0$ as is seen in the figures.

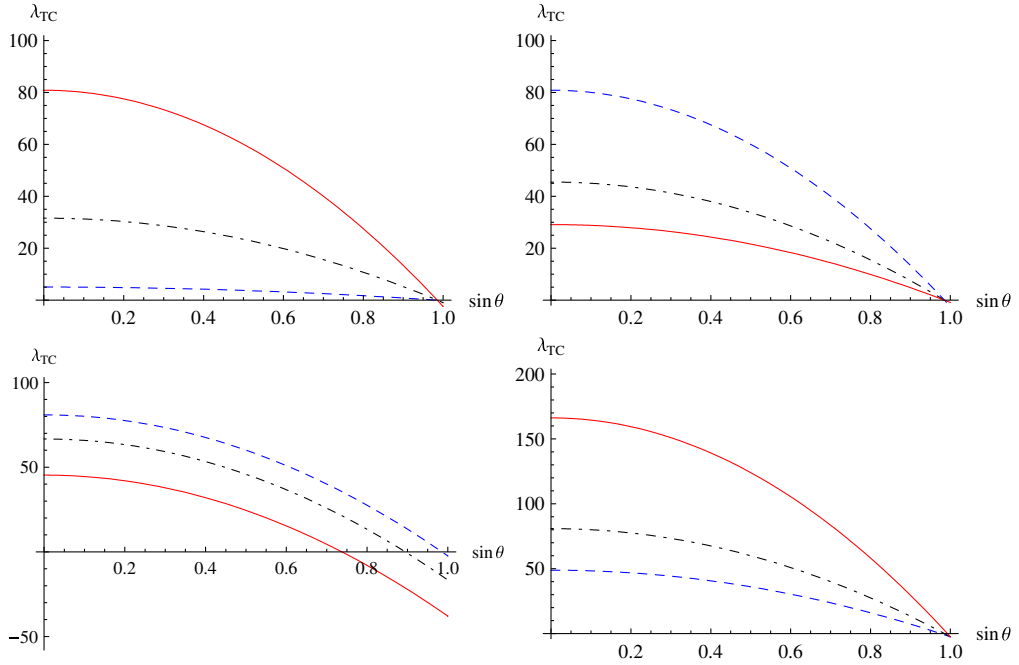

FIG. 3 (color online). Dependence of the quartic TC self-coupling λ_{TC} on the $h\tilde{\sigma}$ mixing s_θ with dashed, dash-dotted, and solid lines corresponding to (i) $g_{TC} = 2, 5, 8$, $M_{\tilde{Q}} = 300$ GeV, $m_{\tilde{\pi}} = 150$ GeV, and $M_{\tilde{\sigma}} = 500$ GeV; (ii) $g_{TC} = 8$, $M_{\tilde{Q}} = 300, 400, 500$ GeV, $m_{\tilde{\pi}} = 150$ GeV, and $M_{\tilde{\sigma}} = 500$ GeV; (iii) $g_{TC} = 8$, $M_{\tilde{Q}} = 300$ GeV, $m_{\tilde{\pi}} = 150, 250, 350$ GeV, and $M_{\tilde{\sigma}} = 500$ GeV; (iv) $g_{TC} = 8$, $M_{\tilde{Q}} = 300$ GeV, $m_{\tilde{\pi}} = 150$ GeV, and $M_{\tilde{\sigma}} = 400, 500, 700$ GeV, in each plot from top to bottom and left to right, respectively. Here and below, $M_h = 125$ GeV. The coupling λ_{TC} is symmetric with respect to $s_\theta \to -s_\theta$.

The λ_H coupling depends only on the s_θ and $M_{\tilde{\sigma}}$, and both λ and λ_H are generally constrained λ, $\lambda_H \lesssim 10$.

In our analysis, for the sake of simplicity and transparency, we wish to employ an analogy with QCD and hadron physics as long as possible, which is reasonable (even though not necessary) since the TC confinement group and technifermion hypercharge are assumed to be the same as for standard quarks. If such an analogy is indeed realized in nature, one would need to pay attention to other possible similarities e.g., in properties of QCD and techni-QCD vacuum subsystems. The QCD vacuum at scales $\Lambda_{QCD} \sim 200$ MeV is formed by gluon and quark condensates [41]:

$$\begin{aligned}\langle 0|\frac{\alpha_s}{\pi}\hat{G}_{\mu\nu}\hat{G}^{\mu\nu}|0\rangle &= (365 \pm 20\ \text{MeV})^4 \simeq (2\Lambda_{QCD})^4,\\ \langle 0|\bar{u}u|0\rangle &= \langle 0|\bar{d}d|0\rangle\\ &= -l_g\langle 0|\frac{\alpha_s}{\pi}\hat{G}_{\mu\nu}\hat{G}^{\mu\nu}|0\rangle\\ &= -(235 \pm 15\ \text{MeV})^3, \end{aligned} \tag{2.22}$$

where $\Lambda_{QCD}^{-1} \simeq 10^{-13}$ sm is the characteristic hadron size, whereas the correlation length $l_g \simeq (1500\ \text{MeV})^{-1}$ is the characteristic length scale of the nonperturbative gluon field fluctuations. In the meson spectrum, the lightest states are pions with mass $m_\pi \simeq 140$ MeV (the pseudo-Goldstone

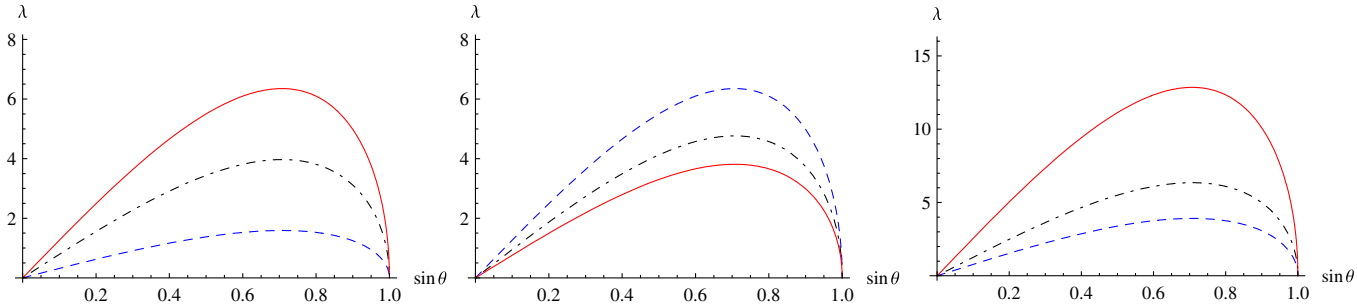

FIG. 4 (color online). Dependence of the quartic Higgs-TC coupling λ on the $h\tilde{\sigma}$ mixing s_θ with dashed, dash-dotted, and solid lines corresponding to (i) $g_{TC} = 2, 5, 8$, $M_{\tilde{Q}} = 300$ GeV, and $M_{\tilde{\sigma}} = 500$ GeV; (ii) $g_{TC} = 8$, $M_{\tilde{Q}} = 300, 400, 500$ GeV, and $M_{\tilde{\sigma}} = 500$ GeV; (iii) $g_{TC} = 8$, $M_{\tilde{Q}} = 300$ GeV, and $M_{\tilde{\sigma}} = 400, 500, 700$ GeV, in each plot from left to right, respectively. It does not depend on $m_{\tilde{\pi}}$. The coupling λ is antisymmetric with respect to $s_\theta \to -s_\theta$.

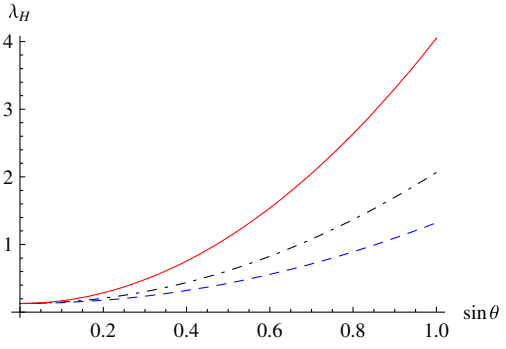

FIG. 5 (color online). Dependence of the quartic Higgs boson self-coupling $\lambda_{\rm H}$ on the $h\tilde{\sigma}$ mixing s_θ with dashed, dash-dotted, and solid lines corresponding to $M_{\tilde{\sigma}} = 400$, 500, and 700 GeV, respectively. It does not depend on other free parameters of the CSTC model. The coupling $\lambda_{\rm H}$ is symmetric with respect to $s_\theta \to -s_\theta$.

modes of the quark condensate excitations) and σ meson $\sigma = f_0(500)$ with mass $m_\sigma \simeq 500$ MeV (the lightest glueball as a collective excitation of the gluon condensate). In the framework of the hypothesis about the technicolor nature of the Higgs vacuum $v \sim 200$ GeV, it is natural to assume that the second techni-QCD vacuum subsystem is formed by a condensate of technigluons and light technifermions at a nearby scale $\Lambda_{\rm TC} \gtrsim 200$ GeV, being therefore, at least, 1000 times higher than the $\Lambda_{\rm QCD}$ scale. Then, a reasonable order-of-magnitude estimate leads to

$$\langle 0|\frac{\alpha_{\rm TC}}{\pi}\hat{F}_{\mu\nu}\hat{F}^{\mu\nu}|0\rangle \sim (2\Lambda_{\rm TC})^4,$$
$$\langle 0|\bar{U}U|0\rangle = \langle 0|\bar{D}D|0\rangle \sim -l_{\rm TC}(2\Lambda_{\rm TC})^4.$$

If the current technifermion masses obey the same hierarchy as that of usual quarks, the lightest technihadron excitations in the bosonic spectrum are technipions $\tilde{\pi}^{0,\pm}$ and technisigma meson $\tilde{\sigma}$, whereas in the fermion spectrum techninucleons P and N. Such a dynamical similarity between color and technicolor enables us to estimate characteristic masses of the lightest technihadrons and constituent technifermions through the scale transformation of ordinary hadron states via scale factor $\zeta = \Lambda_{\rm TC}/\Lambda_{\rm QCD} \gtrsim 1000$, i.e.,

$$\begin{aligned} &m_{\tilde{\pi}} \gtrsim 140 \text{ GeV}, \qquad M_{\tilde{\sigma}} \gtrsim 500 \text{ GeV}, \\ &M_{\tilde{Q}} \gtrsim 300 \text{ GeV}, \qquad M_P \simeq M_N \gtrsim 1 \text{ TeV}, \end{aligned} \tag{2.23}$$

which imply that $m_{\tilde{\pi}} > M_h$, $M_{\tilde{\sigma}} > M_h$, $M_{\tilde{\sigma}} > m_{\tilde{\pi}}$, and $u \gtrsim 100$ GeV for $g_{\rm TC} \simeq 3$. Also, with respect to interactions with known particles at typical 4-momentum squared transfers $Q^2 \ll l_{\rm TC}^{-2} \gtrsim 2.3$ TeV^2, the lightest technihadrons behave as elementary particles, which participate in electroweak interactions only. The technipions are then treated as being in the adjoint representation of the $SU(2)_{\rm W}$ with hypercharge equal to zero, thus justifying what was done above, whereas techninucleons can be included as the fundamental representation of the electroweak group $SU(2)_{\rm W} \otimes U(1)_{\rm Y}$ with hypercharge $Y_{\rm TN} = 1$ along with the constituent technifermion doublet (2.2). Heavy techninucleons, however, are likely to be irrelevant for the LHC phenomenology but can play an important role in astrophysics as a plausible candidate for dark matter. The conditions (2.23) following from the analogy of QCD and techni-QCD will be used below in phenomenological studies in the CSTC framework.

D. The physical Lagrangian of the CSTC model

In this section, we consider the principal part of the physical CSTC Lagrangian relevant for studies of the basic phenomenological processes in the CSTC model, e.g., corrections to EW precision observables, as well as Higgs, technipion, and technisigma production and decays, discussed below.

The vectorlike interactions $\bar{\tilde{Q}}\,\tilde{Q}\,V$ of technifermions and gauge bosons $V = Z^0$, $W^\pm$, γ are given by

$$\begin{aligned} L_{\bar{\tilde{Q}}\tilde{Q}V} = &\frac{1}{\sqrt{2}} g\bar{U}\gamma^\mu D \cdot W_\mu^+ + \frac{1}{\sqrt{2}} g\bar{D}\gamma^\mu U \cdot W_\mu^- \\ &+ \frac{g}{c_W} Z_\mu \sum_{f=U,D} \bar{f}\,\gamma^\mu (t_3^f - q_f s_W^2) f \\ &+ e \sum_{f=U,D} q_f \bar{f}\gamma^\mu A_\mu f, \end{aligned} \tag{2.24}$$

where $e = g s_W$ is the electron charge, t_3^f is the weak isospin ($t_3^U = 1/2$, $t_3^D = -1/2$), and $q_f = Y_{\tilde{Q}}/2 + t_3^f$ is the technifermion charge. As agreed above, we choose $Y_{\tilde{Q}} = 1/3$ in analogy to the SM; thus, $q_U = 2/3$ and $q_D = -1/3$.

The Yukawa-type interactions $\bar{\tilde{Q}}\,\tilde{Q}\,h + \bar{\tilde{Q}}\,\tilde{Q}\,\tilde{\sigma} + \bar{\tilde{Q}}\,\tilde{Q}\,\tilde{\pi}$ of constituent technifermions with scalar (h and $\tilde{\sigma}$) and pseudoscalar ($\pi^{0,\pm}$) fields are driven by

$$\begin{aligned} &L_{\bar{\tilde{Q}}\tilde{Q}h} + L_{\bar{\tilde{Q}}\tilde{Q}\tilde{\sigma}} + L_{\bar{\tilde{Q}}\tilde{Q}\tilde{\pi}} \\ &\quad = -g_{\rm TC}(c_\theta\tilde{\sigma} + s_\theta h)\cdot(\bar{U}U + \bar{D}D) - i\sqrt{2}g_{\rm TC}\tilde{\pi}^+\bar{U}\gamma_5 D \\ &\qquad - i\sqrt{2}g_{\rm TC}\tilde{\pi}^-\bar{D}\gamma_5 U - ig_{\rm TC}\tilde{\pi}^0(\bar{U}\gamma_5 U - \bar{D}\gamma_5 D). \end{aligned} \tag{2.25}$$

As was advocated above, at relatively low energies $\sim$0.1 TeV close to the $M_{\rm EW}$ scale the Lagrangians of the technifermion interactions (2.24) and (2.25) should be used in the loop-induced processes with constituent quarks propagating inside loops only.

The interactions of technipions with gauge bosons which will be used in further calculations are defined as follows:

$$
\begin{aligned}
L_{\tilde{\pi}\tilde{\pi}V} &= igW^{\mu+}\cdot(\tilde{\pi}^0\tilde{\pi}^-_{,\mu}-\tilde{\pi}^-\tilde{\pi}^0_{,\mu})\\
&+ igW^{\mu-}\cdot(\tilde{\pi}^+\tilde{\pi}^0_{,\mu}-\tilde{\pi}^0\tilde{\pi}^+_{,\mu})\\
&+ ig(c_W Z_\mu + s_W A_\mu)\cdot(\tilde{\pi}^-\tilde{\pi}^+_{,\mu}-\tilde{\pi}^+\tilde{\pi}^-_{,\mu})\\
&+ g^2 W^+_\mu W^{\mu-}\cdot(\tilde{\pi}^0\tilde{\pi}^0+\tilde{\pi}^+\tilde{\pi}^-)\\
&+ g^2(c_W Z_\mu + s_W A_\mu)^2\cdot\tilde{\pi}^+\tilde{\pi}^- + \cdots, \qquad (2.26)
\end{aligned}
$$

where $\tilde{\pi}_{,\mu}\equiv\partial_\mu\tilde{\pi}$. All triple and quartic interactions, which are necessary in calculations of technipion contributions to the gauge bosons self-energies, are written down here.

The Yukawa interactions $\bar{f}fh+\bar{f}f\tilde{\sigma}$ of the ordinary fermions get modified compared to the SM:

$$
L_{\bar{f}fh}+L_{\bar{f}f\tilde{\sigma}} = -g(c_\theta h - s_\theta\tilde{\sigma})\cdot\frac{m_f}{2M_W}\bar{f}f. \qquad (2.27)
$$

The Lagrangians of the $h\tilde{\pi}\tilde{\pi}$ and $hWW+hZZ$ interactions are

$$
\begin{aligned}
L_{h\tilde{\pi}\tilde{\pi}} &= -(\lambda_{\rm TC}us_\theta-\lambda v c_\theta)h(\tilde{\pi}^0\tilde{\pi}^0+2\tilde{\pi}^+\tilde{\pi}^-)\\
&= -\frac{M_h^2-m_{\tilde{\pi}}^2}{2M_{\tilde{Q}}}g_{\rm TC}s_\theta h(\tilde{\pi}^0\tilde{\pi}^0+2\tilde{\pi}^+\tilde{\pi}^-),\\
L_{hWW}+L_{hZZ} &= gM_W c_\theta h W^+_\mu W^{\mu-}\\
&+\frac{1}{2}(g^2+g_1^2)^{1/2}M_Z c_\theta h Z_\mu Z^\mu. \qquad (2.28)
\end{aligned}
$$

The Lagrangians of the $\tilde{\sigma}\tilde{\pi}\tilde{\pi}$ and $\tilde{\sigma}WW+\tilde{\sigma}ZZ$ interactions are

$$
\begin{aligned}
L_{\tilde{\sigma}\tilde{\pi}\tilde{\pi}} &= -(\lambda_{\rm TC}uc_\theta+\lambda v s_\theta)\tilde{\sigma}(\tilde{\pi}^0\tilde{\pi}^0+2\tilde{\pi}^+\tilde{\pi}^-)\\
&= -\frac{M_{\tilde{\sigma}}^2-m_{\tilde{\pi}}^2}{2M_{\tilde{Q}}}g_{\rm TC}c_\theta\tilde{\sigma}(\tilde{\pi}^0\tilde{\pi}^0+2\tilde{\pi}^+\tilde{\pi}^-),\\
L_{\tilde{\sigma}WW}+L_{\tilde{\sigma}ZZ} &= -gM_W s_\theta\tilde{\sigma}W^+_\mu W^{\mu-}\\
&-\frac{1}{2}(g^2+g_1^2)^{1/2}M_Z s_\theta\tilde{\sigma}Z_\mu Z^\mu. \qquad (2.29)
\end{aligned}
$$

The Lagrangian of quartic scalar-gauge $(\tilde{\sigma}/h)^2VV$ interactions is given by

$$
\begin{aligned}
L_{(\tilde{\sigma}/h)^2VV} &= \frac{1}{4}(c_\theta h - s_\theta\tilde{\sigma})^2\\
&\cdot\left(g^2W^+_\mu W^{\mu-}+\frac{1}{2}(g^2+g_1^2)Z^\mu Z_\mu\right). \qquad (2.30)
\end{aligned}
$$

E. Nearly conformal limit: The minimal CSTC

In the SM, the arbitrary quadratic terms with the "wrong" sign in the Higgs potential are usually required for the classical (nonquantum) Higgs mechanism of the EWSB. As we have noticed above, in the framework of the CSTC model there is a possibility for another interpretation of the Higgs mechanism in which the nature of all energy scales (including the Higgs VEV) is quantum topological. Let us look into the latter possibility in detail.

In the rigorous QCD framework, there is not any fundamental scalar sector, and thus scalar μ terms do not appear. In the theory of nonperturbative QCD vacuum, all the scale parameters have a quantum-topological nature and are expressed through the gluon condensate $\langle GG\rangle$ and the correlation length l_g, whereas the quark condensate $\langle q\bar{q}\rangle$ is induced by the gluon one (2.22). Clearly, low-energy hadron physics based upon the effective GLσM should reproduce the nonperturbative QCD predictions. On the other hand, it is well known that, in the limit of small current quark masses $m_q\to 0$ (the chiral limit), the QCD Lagrangian restores the conformal symmetry. Similarly, the σ model as an effective model of nonperturbative QCD should obey the conformal symmetry in the chiral QCD limit. In this case, the μ_S term corresponding to the σ field is forbidden by the conformal symmetry. In a realistic case, the conformal symmetry in QCD is broken due to nonzeroth current quark masses. However, the current up- and down-quark masses are small compared to the value of the quark condensate $\langle q\bar{q}\rangle$ or, equivalently, the pion mass, i.e., $m_{u,d}\ll m_\pi$, so it is meaningful to assume that an induced μ_S term, if it exists, should also be small $\mu_S\ll m_\pi$. In this case, since $\langle GG\rangle$, $\langle q\bar{q}\rangle$, and small current masses $m_{u,d}\ll m_\pi$ are the only physical parameters in nonperturbative QCD, the σ VEV $u\sim m_\pi$ has a quantum-topological nature, so it should be expressed only through these parameters and given by e.g., $\langle q\bar{q}\rangle$ or, equivalently, m_π. Of course, this logic is rather naive, since the σ model does not have the status of a fundamental theory but rather serves as an effective low-energy phenomenological model with its own limitations and constraints. Note that a dynamical theory of the QCD vacuum does not exist yet, our understanding of nonperturbative effects is very limited, and one cannot make any strong claims here.

The above line of naive arguments can be naturally extended to the technifermion sector in confinement by adopting a direct analogy between nonperturbative QCD and techni-QCD. Looking at Eqs. (2.9), we notice that for not very large scalar self-couplings $|\lambda|, |\lambda_{\rm TC}|, \lambda_{\rm H}\sim 0.1$–$10$ in the potential (2.8), the technisigma VEV u can be expressed through the technifermion condensate, or $m_{\tilde{\pi}}$, for small $\mu_S\ll m_{\tilde{\pi}}$, which can be valid in the nearly conformal limit of chiral techni-QCD $m_{U,D}\ll m_{\tilde{\pi}}$ if and only if the Higgs boson VEV is also small compared to the techniconfinement scale, i.e., $\mu_{\rm H}\ll m_{\tilde{\pi}}$. The latter means that both the vacua, the Higgs and technisigma VEVs, have the same quantum-topological nature and are completely determined by the technifermion condensate. This theoretically appealing scenario would be rigorous and strictly valid in the exact chiral techni-QCD limit with vanishing current technifermion masses $m_{U,D}\to 0$. In the nearly conformal limit, there is a weak or no running of the strong techni-QCD coupling. This is in accordance with the analytic QCD (see e.g., Ref. [42]) or other phenomenological

approaches predicting a rather slow bounded or even "frozen" behavior of the strong QCD coupling in the infrared domain, while nonperturbative QCD contributions are strongly dominated over the perturbative ones in the constituent quark-meson interactions at small Q^2. To this end, in the nearly conformal limit, all the μ terms can be neglected in the Lagrangian (2.8) without affecting the SM Higgs mechanism itself, which then would be triggered completely by the technifermion condensate, giving rise to even more restricted parameter space of the model. Let us look into this nontrivial possibility, which is simply a particular case of the more general CSTC model described above, in some more detail.

The solutions of the two tadpole equations (2.10) can then be written with respect to VEVs as follows:

$$u = \left(\frac{\lambda_{\rm H}}{\delta}\right)^{1/3} \bar{g}_{\rm TC}^{1/3}, \qquad v = \left(\frac{\xi\lambda}{\lambda_{\rm H}}\right)^{1/2}\left(\frac{\lambda_{\rm H}}{\delta}\right)^{1/3} \bar{g}_{\rm TC}^{1/3}, \tag{2.31}$$

where $\delta = \lambda_{\rm H}\lambda_{\rm TC} - \lambda^2$, $\bar{g}_{\rm TC} = g_{\rm TC}|\langle\bar{\tilde{Q}}\,\tilde{Q}\rangle| > 0$, and the sign factor $\xi = \mathrm{sgn}(M_{\tilde{\sigma}}^2 - 3m_{\tilde{\pi}}^2)$ such that $\xi\lambda \equiv |\lambda| \geq 0$ and $\lambda_H > 0$ always. From relations (2.31), it follows that both VEVs (and hence both the EWSB and the chiral symmetry breaking) are induced by the technifermion condensate since $u, v \sim |\langle\bar{\tilde{Q}}\,\tilde{Q}\rangle|^{1/3}$. So, our choice of the potential part of the TC Lagrangian L_U (2.8) provides a physically interesting interpretation of the Higgs vacuum condensate as triggered by the technifermion condensate $\langle\bar{\tilde{Q}}\,\tilde{Q}\rangle \neq 0$ at low scales $\sim$0.1 TeV.

It is convenient to redefine yet unknown parameters, the technisigma VEV, u, and $\bar{g}_{\rm TC}$ in terms of the Higgs VEV, v, and scalar self-couplings λ, $\lambda_{\rm H}$, $\lambda_{\rm TC}$ as follows:

$$u = v\cdot\left(\frac{\lambda_{\rm H}}{\xi\lambda}\right)^{1/2}, \qquad \bar{g}_{\rm TC} = v^3\left(\frac{\lambda_{\rm H}\lambda_{\rm TC}}{\lambda} - \lambda\right)\cdot\left(\frac{\lambda_{\rm H}}{\xi\lambda}\right)^{1/2}. \tag{2.32}$$

The technipion mass is given by

$$m_{\tilde{\pi}}^2 = v^2\left(\frac{\lambda_H\lambda_{\rm TC}}{\lambda} - \lambda\right), \qquad m_{\tilde{\pi}} \sim v. \tag{2.33}$$

Note that, in the limit $M_{\tilde{\sigma}} \to \sqrt{3}m_{\tilde{\pi}}$, we have $\delta \sim \lambda \to 0$, whereas $\bar{g}_{\rm TC} \sim u \sim M_{\tilde{Q}} \sim 1/\sqrt{|\lambda|} \to \infty$ at finite $m_{\tilde{\pi}}$ and v. Also, $s_\theta \to 0$ in this case, so h and $\tilde{\sigma}$ do not mix ("no $h\tilde{\sigma}$-mixing" limit). This peculiar limit physically corresponds to decoupling of the technifermion condensate (and hence the techniconfinement scale $\Lambda_{\rm TC}$) up to very high scales, while providing light technipions and technisigma in the spectrum and the TC-induced EWSB mechanism in the usual way. Of course, the formal mathematical singularities corresponding to a very large techniconfinement scale $\Lambda_{\rm TC}$, or, equivalently, large u and $|\langle\bar{\tilde{Q}}\,\tilde{Q}\rangle|$ (see Fig. 7 below), should be regularized by yet unknown high-scale TC physics, and thus vicinities of these special points are to be excluded from the current consideration. Interestingly enough, the Higgs boson turns out to be absolutely standard close to the singular points—its properties are not affected by the extra TC degrees of freedom, since corresponding new TC-induced couplings vanish in this case at $M_{\tilde{\sigma}} \to \sqrt{3}m_{\tilde{\pi}}$. While physically possible, this peculiar situation, however, is not realized if one adopts the naive scaling between the QCD and techni-QCD considered in this analysis. The absence of any deviations from the SM in the measured Higgs boson properties, from the point of view of the minimal CSTC discussed here, would then mean physically that the no $h\tilde{\sigma}$-mixing scenario is realized in nature, but this does not rule out the TC-induced EWSB mechanism (see below).

The mass form of the physical scalars, h and $\tilde{\sigma}$ fields, can be represented by the following matrix:

$$M_{h\tilde{\sigma}} = \begin{pmatrix} 3m_{\tilde{\pi}}^2 + 2\lambda v^2 & -2v^2\sqrt{\xi\lambda\lambda_H} \\ -2v^2\sqrt{\xi\lambda\lambda_H} & 2\lambda_H v^2 \end{pmatrix}. \tag{2.34}$$

The diagonalization of this matrix leads to masses of the physical states scalar states, i.e.,

$$M_{\tilde{\sigma},h}^2 = \frac{1}{2}v^2\left\{\left(2\lambda_H + 2\lambda + 3\frac{m_{\tilde{\pi}}^2}{v^2}\right) \pm \sqrt{\left(2\lambda_H + 2\lambda + 3\frac{m_{\tilde{\pi}}^2}{v^2}\right)^2 + 16\lambda\lambda_H}\right\}. \tag{2.35}$$

Then, the $h\tilde{\sigma}$-mixing angle is given by

$$c_\theta = \left(1 + \frac{(M_{\tilde{\sigma}}^2 - m_{11})^2}{m_{12}^2}\right)^{-1/2}, \qquad s_\theta = \xi\sqrt{1 - c_\theta^2}, \tag{2.36}$$

where $m_{11} = (M_{h\tilde{\sigma}})_{11}$ and $m_{12} = (M_{h\tilde{\sigma}})_{12}$ are the elements of the mass matrix (2.34). In the analysis of the parameter space, it is again convenient to express free scalar self-couplings $\{\lambda, \lambda_{\rm H}, \lambda_{\rm TC}\}$ through the physical masses $\{m_{\tilde{\pi}}^2, M_{\tilde{\sigma}}^2, M_h^2\}$:

$$\lambda = \frac{3m_{\tilde{\pi}}^2(M_{\tilde{\sigma}}^2 + M_h^2) - M_{\tilde{\sigma}}^2M_h^2 - 9m_{\tilde{\pi}}^4}{6v^2m_{\tilde{\pi}}^2}, \qquad \lambda_{\rm H} = \frac{M_{\tilde{\sigma}}^2M_h^2}{6v^2m_{\tilde{\pi}}^2}, \qquad \lambda_{\rm TC} = \frac{\lambda}{\lambda_{\rm H}}\left(\lambda + \frac{m_{\tilde{\pi}}^2}{v^2}\right). \tag{2.37}$$

By fixing the Higgs boson mass to its recently measured value $M_h \simeq 125$ GeV, one further reduces the freedom down to three free parameters only, $\{m_{\tilde{\pi}}, M_{\tilde{\sigma}}, M_{\tilde{Q}}\}$, compared to five parameters in the nonminimal case (cf. Sec. II C). Note that the scalar self-couplings and the mixing angle θ depend only on two parameters $\{m_{\tilde{\pi}}, M_{\tilde{\sigma}}\}$, whereas $M_{\tilde{Q}}$ can be used to define $g_{\rm TC}$ or $\langle\bar{\tilde{Q}}\,\tilde{Q}\rangle$.

In Fig. 6, we have presented plots of the sine of the mixing angle $s_\theta = s_\theta(m_{\tilde{\pi}}, m_{\tilde{\sigma}})$ and scalar self-couplings—Higgs-(pseudo)scalar coupling $\lambda = \lambda(m_{\tilde{\pi}}, m_{\tilde{\sigma}})$, quartic Higgs self-coupling $\lambda_{\rm H} = \lambda_{\rm H}(m_{\tilde{\pi}}, m_{\tilde{\sigma}})$, and (pseudo)scalar self-coupling $\lambda_{\rm TC} = \lambda_{\rm TC}(m_{\tilde{\pi}}, m_{\tilde{\sigma}})$. At relatively large technipion masses $m_{\tilde{\pi}} \gtrsim 250$ GeV, the $h\tilde{\sigma}$ mixing becomes rather small, $s_\theta \lesssim 0.2$, while it does not

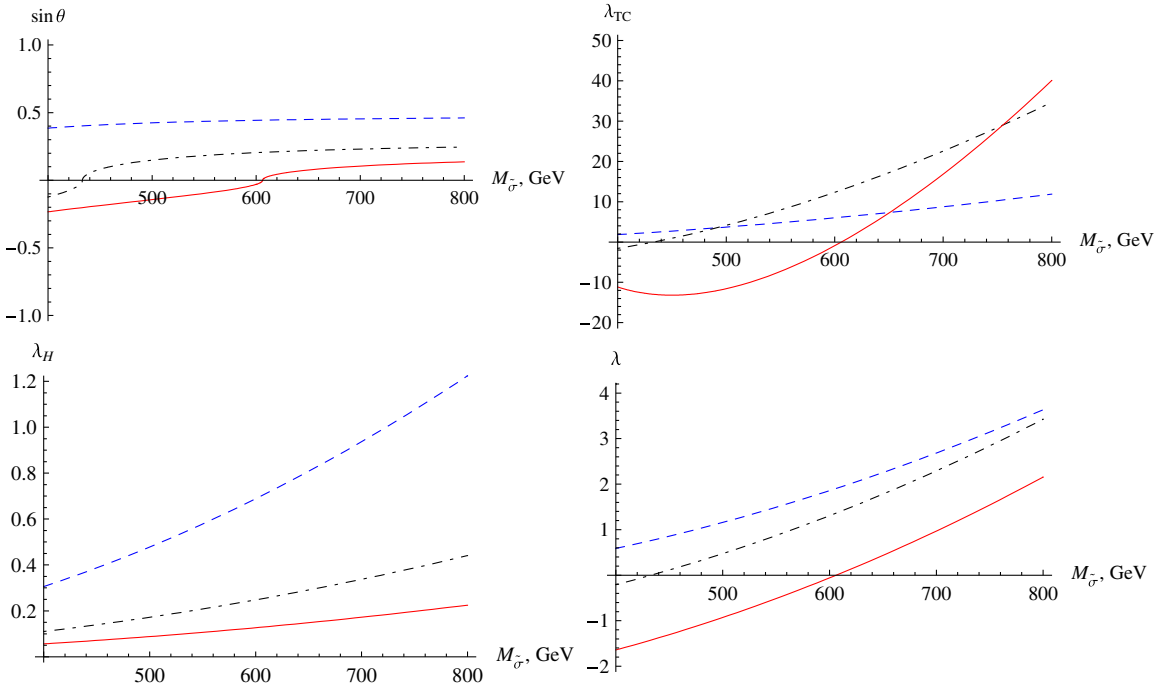

FIG. 6 (color online). Dependence of the $h\tilde{\sigma}$ mixing s_θ and the Higgs/TC self-couplings $\lambda_{\rm TC}$, $\lambda_{\rm H}$, and λ on $M_{\tilde{Q}}$ in the minimal CSTC scenario with dashed, dash-dotted, and solid lines corresponding to $m_{\tilde{\pi}} = 150$, 250, and 350 GeV, respectively. The no $h\tilde{\sigma}$-mixing limit corresponds to zeros of the curves at $M_{\tilde{\sigma}} = \sqrt{3}m_{\tilde{\pi}}$.

strongly depend on the technisigma mass, away from "no-mixing" points. As was noticed above, the condition $\lambda = 0$ (or $s_\theta = 0$) corresponds to the no-mixing limit and is represented by a relation on masses: $M_{\tilde{\sigma}} = \sqrt{3}m_{\tilde{\pi}}$. In the considered ranges of masses, the values of λ and $\lambda_{\rm H}$ do not exceed a few units, so they are of the order of strong ("fat") couplings in usual hadron dynamics (e.g., $g_{\rho\pi\pi} \sim$ 5–6) and gradually increase at large $M_{\tilde{\sigma}}$. The (pseudo) scalar self-coupling $\lambda_{\rm TC}$ can reach larger values $\sim$100 at large values of $M_{\tilde{\sigma}} \gtrsim 800$ GeV, restricting the allowable region of physical parameters and applicability of the GLTσM under consideration. Experimental information on the scalar self-couplings λ and $\lambda_{\rm TC}$ would shed light on the true origin of the Higgs mechanism, making it possible to determined which minimal or nonminimal CSTC scenario is realized in nature.

In Fig. 7, we show the dimensionless $\bar{g}_{\rm TC}/v^3$ (left) and $\tilde{\sigma}$ VEV u (right) parameters with respect to $M_{\tilde{\sigma}}$ for different values of $m_{\tilde{\pi}}$ in the minimal CSTC scenario. The technisigma VEV $u = u(m_{\tilde{\pi}}, m_{\tilde{\sigma}})$ can be smaller than the Higgs VEV v, $u \lesssim v$, almost in all physically favorable regions of parameter space where $m_{\tilde{\pi}} \sim v$, except for vicinities of no $h\tilde{\sigma}$-mixing points $M_{\tilde{\sigma}} \simeq \sqrt{3}m_{\tilde{\pi}}$ where u can be larger or even much larger than the Higgs VEV v. The latter case can be interesting both theoretically and phenomenologically in the case of the absence of any deviations of Higgs

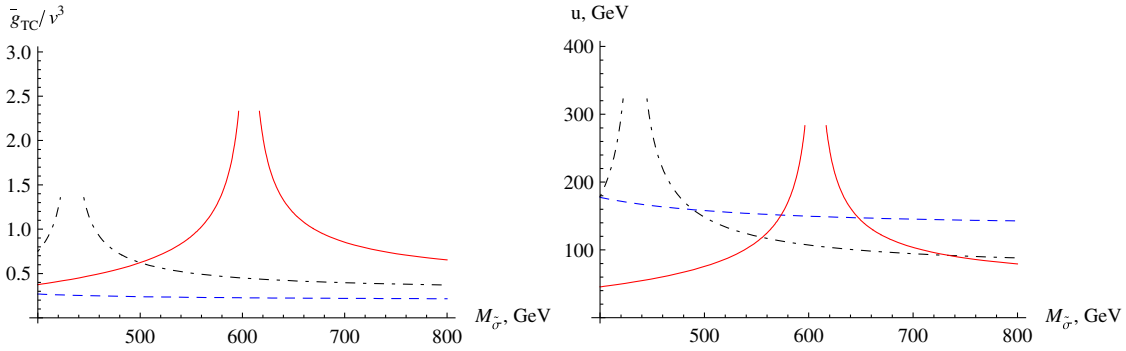

FIG. 7 (color online). The dimensionless $\bar{g}_{\rm TC}/v^3$ (left) and $\tilde{\sigma}$ VEV u (right) parameters with respect to $M_{\tilde{\sigma}}$ in the minimal CSTC scenario with dashed, dash-dotted, and solid lines corresponding to $m_{\tilde{\pi}} = 150$, 250, and 350 GeV, respectively. The no $h\tilde{\sigma}$-mixing limit corresponds to positions of the singularities on the curves at $M_{\tilde{\sigma}} = \sqrt{3}m_{\tilde{\pi}}$, and the vicinity of those are excluded from the plots.

boson properties from the SM predictions at the LHC. Then, the only source of new information about the TC sector can come from measurements of the Higgs boson scalar self-couplings and possible technipion and technisigma phenomenology.

One should notice here that if the small $h\tilde{\sigma}$-mixing scenario with $s_\theta \to 0$ and $\lambda \to 0$ is realized in nature, we have the technicolor decoupling regime with large $u \gg v$ and hence $\Lambda_{\rm TC} \sim M_{\tilde{Q}} \gg M_{\rm EW}$, while the Higgs boson, technipions, and technisigma remain at the EW scale according to the tree-level mass formulas of the model. Remarkably enough, the Higgs VEV is still expressed in terms of the technifermion condensate by Eq. (2.31) for vanishingly small but nonzeroth $\lambda \neq 0$ preserving the dynamical nature of the EWSB (or effective Higgs) mechanism.

III. ELECTROWEAK CONSTRAINTS ON THE CSTC

A. Oblique corrections

The effects of heavy new physics (NP) particles of various types onto Z^0 and $W^\pm$ observables (e.g., masses and widths) typically emerging through extra loop contributions to Z^0, $W^\pm$, and γ (diagonal and nondiagonal) self-energies can be parameterized by means of the so-called oblique corrections or Peskin-Takeuchi (PT) parameters [14]. The first three of these parameters S, T, and U are normally introduced in the limiting case of large masses of new particles compared to the EW scale, i.e., in the limit $M_{\rm EW}/M_{\rm NP} \ll 1$ ($M_{\rm NP}$ is the NP scale). If one relaxes this assumption, the S, T, U parameters get somewhat modified, and an additional three independent parameters denoted as V, W, and X are introduced (see e.g., Refs. [43,44]). The oblique corrections are rather strongly constrained by the EW precision measurements [45]

$$S = 0.00^{+0.11}_{-0.10}, \qquad T = 0.02^{+0.11}_{-0.12}, \qquad U = 0.08 \pm 0.11 \tag{3.1}$$

and must be respected by realistic NP models (for existing constraints on higher V, W, X parameters, see e.g., Ref. [46]). The extensive studies of these constraints are very critical for all existing TC models. In particular, some of the traditional TC scenarios are currently being ruled out or are in a considerable tension with constraints on S, T, U parameters [14] (see also Refs. [15,16]). Let us analyze these constraints in the suggested CSTC scenario.

The analysis we present further in this section does not depend on whether one includes $\mu_{S,H}$ terms or not; the difference between these nonminimal and minimal versions of the CSTC model can be crucial only for processes with (pseudo)scalar self-couplings, which can be important, e.g., for Higgs and technipion phenomenology.

In the earlier sections, we have established the phenomenologically reasonable intervals for masses and couplings of new TC particles (technipions, technisigma, and constituent technifermions) based on analogies with ordinary QCD and hadron physics together with the relative proximity of the new TC scale $\Lambda_{\rm TC} \sim 0.1$–$1$ TeV. In what follows, these regions of parameter space will be tested against the EW precision constraints given by Eq. (3.1).

The generic definitions of the PT parameters are given in terms of corrections to the vacuum polarization functions $\delta\Pi_{\rm XY}(q^2)$ of the gauge bosons (X, Y = W, Z, γ) coming either from new particles, additional to those in the SM, $\Pi^{\rm new}_{\rm XY}(q^2)$, or from a modification of the SM parameters due to NP effects, $\Pi^{\rm SM'}_{\rm XY}(q^2)$, i.e.,

$$\begin{aligned} \delta\Pi_{\rm XY}(q^2) &\equiv \Pi^{\rm NP}_{\rm XY}(q^2) - \Pi^{\rm SM}_{\rm XY}(q^2), \\ \Pi^{\rm NP}_{\rm XY}(q^2) &= \Pi^{\rm new}_{\rm XY}(q^2) + \Pi^{\rm SM'}_{\rm XY}(q^2). \end{aligned} \tag{3.2}$$

The expressions for the S, T, U parameters in terms of generic polarization functions $\delta\Pi_{\rm XY}(q^2)$ and their derivatives $\delta\Pi'_{\rm XY}(q^2) = d\delta\Pi/dq^2$ calculated beyond the linear approximation in q^2 variable read [43,44]

$$\begin{aligned} \frac{\alpha}{4s_W^2 c_W^2} S &= \frac{\delta\Pi_{ZZ}(M_Z^2) - \delta\Pi_{ZZ}(0)}{M_Z^2} - \frac{c_W^2 - s_W^2}{c_W s_W}\delta\Pi'_{Z\gamma}(0) \\ &\quad - \delta\Pi'_{\gamma\gamma}(0), \\ \alpha T &= \frac{\delta\Pi_{WW}(0)}{M_W^2} - \frac{\delta\Pi_{ZZ}(0)}{M_Z^2}, \\ \frac{\alpha}{4s_W^2} U &= \frac{\delta\Pi_{WW}(M_W^2) - \delta\Pi_{WW}(0)}{M_W^2} \\ &\quad - c_W^2 \frac{\delta\Pi_{ZZ}(M_Z^2) - \delta\Pi_{ZZ}(0)}{M_Z^2} - s_W^2 \delta\Pi'_{\gamma\gamma}(0) \\ &\quad - 2c_W s_W \delta\Pi'_{Z\gamma}(0). \end{aligned} \tag{3.3}$$

Note that, in the limit $\zeta = M_{\rm EW}/\Lambda_{\rm TC} \ll 1$, we have

$$\frac{\delta\Pi_{WW}(M_Z^2) - \delta\Pi_{WW}(0)}{M_Z^2} = \frac{\delta\Pi_{WW}(M_W^2) - \delta\Pi_{WW}(0)}{M_W^2} + \mathcal{O}(M_{\rm EW}^4/\Lambda_{\rm TC}^4), \tag{3.4}$$

$$\frac{\delta\Pi_{\rm XY}(q^2) - \delta\Pi_{\rm XY}(0)}{q^2} = \delta\Pi'_{\rm XY}(0) + \mathcal{O}(q^4/\Lambda_{\rm TC}^4), \tag{3.5}$$

which are equivalent to working in the linear order in q^2 in power expansions of the polarization functions $\delta\Pi_{\rm XY}(q^2)$. In fact, applying approximate relation (3.5) to expressions (3.3) at $q^2 = M_Z^2$ and having in mind that $\delta\Pi_{Z\gamma}(0) = \delta\Pi_{\gamma\gamma}(0) = 0$ in a realistic case, one arrives at the Particle Data Group formulas [see Eq. (10.65b,c) in Ref. [45]]. We, however, do not assume smallness of ζ in calculations (unless noted otherwise), since the new TC scale $\Lambda_{\rm TC}$ can be rather close to the electroweak scale $M_{\rm EW}$ since they may have the same physical nature in the considered CSTC scenario, and therefore rigorous definitions (3.3) should be applied.

The other three parameters which appear beyond the linear order in q^2 in addition to S, T, and U are defined as follows [43,44]:

$$\alpha V = \delta\Pi'_{ZZ}(M_Z^2) - \frac{\delta\Pi_{ZZ}(M_Z^2) - \delta\Pi_{ZZ}(0)}{M_Z^2},$$
$$\alpha W = \delta\Pi'_{WW}(M_W^2) - \frac{\delta\Pi_{WW}(M_W^2) - \delta\Pi_{WW}(0)}{M_W^2}, \quad (3.6)$$
$$\alpha X = -s_W c_W\left[\frac{\delta\Pi_{Z\gamma}(M_Z^2)}{M_Z^2} - \delta\Pi'_{Z\gamma}(0)\right].$$

In the framework of the CSTC model, the new contributions to W, Z, and γ vacuum polarizations come from technipion, constituent technifermions, and technisigma loops, i.e.,

$$\Pi^{\rm new}_{\rm XY}(q^2) = \Pi^{\tilde\pi}_{\rm XY}(q^2) + \Pi^{\tilde Q}_{\rm XY}(q^2) + \Pi^{\tilde\sigma}_{\rm XY}(q^2), \quad (3.7)$$

while the SM modified contributions come only from the Higgs boson due to modified hVV couplings, $\Pi^h_{\rm XY}(q^2)$, whereas other SM couplings are not changed in the CSTC model; thus, we have

$$\Pi^{\rm SM'}_{\rm XY}(q^2) = \Pi^h_{\rm XY}(q^2). \quad (3.8)$$

The corresponding diagrams are presented in Fig. 8.

Note that the modified Higgs contribution to the gauge boson polarization functions $\Pi^h_{\rm XY}(q^2, M_h^2)$ can be obtained by multiplying the corresponding SM result presented many times in the literature (see e.g., Ref. [47]), $\Pi^{\rm SM,h}_{\rm XY}(q^2, M_h^2)$, by a factor of c_θ^2. Also, the extra contribution due to the $\tilde\sigma$ meson, $\Pi^{\tilde\sigma}_{\rm XY}(q^2, M_{\tilde\sigma}^2)$, can be easily obtained from the Higgs boson one, $\Pi^h_{\rm XY}(q^2, M_h^2)$, by a replacement $c_\theta \to s_\theta$ and $M_h \to M_{\tilde\sigma}$ in corresponding polarization functions [cf. Eqs. (2.28) and (2.29)]. Therefore, the total contribution of the scalar states $\delta\Pi^{\rm sc}_{\rm XY}(q^2)$ to the total $\delta\Pi_{\rm XY}(q^2)$ defined in Eq. (3.2) reads

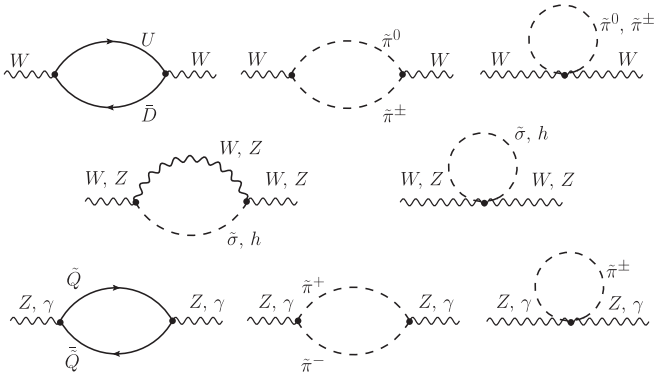

FIG. 8. The additional new (via $\tilde\pi$, $\tilde Q$, and $\tilde\sigma$) and modified (via Higgs boson h) contributions to the gauge bosons Z^0, $W^\pm$, and γ vacuum polarization functions $\delta\Pi_{\rm XY}(q^2)$.

$$\delta\Pi_{\rm XY}(q^2) = \delta\Pi^{\rm sc}_{\rm XY}(q^2) + \Pi^{\tilde\pi}_{\rm XY}(q^2, m_{\tilde\pi}^2) + \Pi^{\tilde Q}_{\rm XY}(q^2, M_{\tilde Q}^2), \quad (3.9)$$

$$\delta\Pi^{\rm sc}_{\rm XY}(q^2) = \Pi^{\tilde\sigma}_{\rm XY}(q^2, M_{\tilde\sigma}^2) + \Pi^h_{\rm XY}(q^2, M_h^2) - \Pi^{\rm SM,h}_{\rm XY}(q^2, M_h^2)$$
$$= s_\theta^2\Pi^{\rm SM,h}_{\rm XY}(q^2, M_{\tilde\sigma}^2) - s_\theta^2\Pi^{\rm SM,h}_{\rm XY}(q^2, M_h^2). \quad (3.10)$$

Apparently, $\delta\Pi^{\rm sc}_{\rm XY}(q^2) \to 0$ and hence the corresponding contributions to the oblique corrections (3.3) and (3.6) turn to zero in the limit of degenerated $\tilde\sigma$ and h masses, $M_{\tilde\sigma} \to M_h$. Also, the function $\delta\Pi^{\rm sc}_{\rm XY}(q^2)$ vanishes in the no $\tilde\sigma h$-mixing limit, when $s_\theta \to 0$, so the corresponding oblique corrections can be very small and fit the EW precision data without a significant tension.

Finally, consider the new contributions coming from $\tilde\pi$ and $\tilde Q$ loops. For illustration, below we show analytical results for the limiting no $h\tilde\sigma$-mixing scenario and degenerated technifermions implying that their constituent masses are equal $M_U = M_D \equiv M_{\tilde Q}$, while forthcoming numerical results and figures will be presented also for the general case with $M_U \neq M_D$ and an arbitrary mixing angle. Note that if one employs an analogy with hadron physics, where the nonperturbative QCD contribution to the constituent masses of up and down quarks is much larger than their current masses, the approximate degeneracy $M_U \simeq M_D$ (or, more precisely, $\Delta M_{\tilde Q} \equiv M_D - M_U \ll M_U, M_D$) is physically reasonable and justified.

Then, the technipion and technifermion contributions can be represented in the following generic form:

$$\Pi^{\tilde\pi}_{\rm XY}(q^2, m_{\tilde\pi}^2) = \frac{g^2}{24\pi^2}K_{\rm XY}F_{\tilde\pi}(q^2, m_{\tilde\pi}^2),$$
$$\Pi^{\tilde Q}_{\rm XY}(q^2, M_{\tilde Q}^2) = \frac{g^2 N_c}{24\pi^2}K_{\rm XY}\kappa_{\rm XY}F_{\tilde Q}(q^2, M_{\tilde Q}^2), \quad (3.11)$$

where $N_{\rm TC} = 3$ is the number of technicolors, coefficients $K_{\rm XY}$ and $\kappa_{\rm XY}$ are shown for two different cases with $Y_{\tilde Q} = 0$ and $Y_{\tilde Q} = 1/3$ in Table I, and momentum-dependent parts are defined as

TABLE I. Summary of coefficients $K_{\rm XY}$ and $\kappa_{\rm XY}$ in gauge boson self-energies X, Y = Z^0, $W^\pm$, γ coming from $\tilde\pi$ and $\tilde Q$ loops (3.11). Two different cases for technifermion hypercharges are considered.

K, κ	WW	ZZ	$\gamma\gamma$	$Z\gamma$
$K_{\rm XY}$	1	c_W^2	s_W^2	$c_W s_W$
$\kappa_{\rm XY}$, $Y_{\tilde Q} = 0$	1	1	1	1
$\kappa_{\rm XY}$, $Y_{\tilde Q} = 1/3$	1	$1 + s_W^4/9c_W^4$	10/9	$1 - s_W^2/9c_W^2$

$$F_{\tilde{\pi}}(q^2, m_{\tilde{\pi}}^2) = \frac{1}{3}q^2 - 2m_{\tilde{\pi}}^2 + 2A_0(m_{\tilde{\pi}}^2) + \frac{1}{2}(q^2 - 4m_{\tilde{\pi}}^2)B_0(q^2, m_{\tilde{\pi}}^2, m_{\tilde{\pi}}^2),$$

$$F_{\tilde{Q}}(q^2, M_{\tilde{Q}}^2) = -\frac{1}{3}q^2 + 2M_{\tilde{Q}}^2 - 2A_0(M_{\tilde{Q}}^2) + (q^2 + 2M_{\tilde{Q}}^2)B_0(q^2, M_{\tilde{Q}}^2, M_{\tilde{Q}}^2),$$

where $A_0(m^2)$ and $B_0(q^2, m^2, m^2)$ are the standard one- and two-point functions [48], respectively. Furthermore, one evaluates these functions and their derivatives for a given set of arguments and substitutes them into Eq. (3.11) and then to Eq. (3.9). By using the relations

$$B_0(0, m^2, m^2) = \frac{A_0(m^2)}{m^2} - 1,$$

$$A_0(m^2) = m^2\left(\frac{1}{\bar{\varepsilon}} + 1 - \ln\frac{m^2}{\mu^2}\right),$$

it can be checked directly that $F_{\tilde{\pi}}(0, m_{\tilde{\pi}}^2) = 0$ and $F_{\tilde{Q}}(0, M_{\tilde{Q}}^2) = 0$, which means that technipions and degenerated technifermions do not contribute to the T parameter, i.e., $T^{\tilde{\pi}} = T^{\tilde{Q}} = 0$ automatically. The only contribution to the T parameter comes from the scalar sector of the theory: $\tilde{\sigma}$ loops and modified Higgs loops given by Eq. (3.10).

The S and U parameter calculation becomes especially transparent if one works in the linear order in q^2 power expansion and applies the approximate relation (3.5). For this purpose, let us consider the simplest case of degenerated technifermion sector with $Y_{\tilde{Q}} = 0$. Then, having $\Pi_{\mathrm{XY}}^{\tilde{\pi}}(0, m_{\tilde{\pi}}^2) = 0$ and $\Pi_{\mathrm{XY}}^{\tilde{Q}}(0, m_{\tilde{Q}}^2) = 0$ for any X, Y, we observe that the $\tilde{\pi}$ and $\tilde{Q}$ contributions to S and U parameters also vanish for $Y_{\tilde{Q}} = 0$ in the linear order in q^2. Indeed, using the corresponding K_{XY} and κ_{XY} coefficients from Table I, we explicitly see that

$$\frac{\alpha S^{\tilde{\pi}+\tilde{Q}}}{4s_W^2c_W^2} = f(M_Z^2, m_{\tilde{\pi}}^2, M_{\tilde{Q}}^2)\cdot\left[c_W^2 - \frac{c_W^2 - s_W^2}{c_W s_W}\cdot c_W s_W - s_W^2\right] = 0,$$

$$\frac{\alpha U^{\tilde{\pi}+\tilde{Q}}}{4s_W^2} = f(M_Z^2, m_{\tilde{\pi}}^2, M_{\tilde{Q}}^2)\cdot[1 - c_W^4 - s_W^4 - 2c_W^2s_W^2] = 0,$$

where $f(m_1^2, m_2^2, m_3^2)$ is some finite regular function of the respective mass scales. We summarize that the only contribution to the S, T, U parameters (in the simplest scenario with $Y_{\tilde{Q}} = 0$ and in the linear order in q^2) comes from scalar loops given by Eq. (3.10). This result is different from traditional TC-based scenarios with chiral-nonsymmetric weak interactions, where S parameters do not vanish and are equal to a relatively large constant, even in the limit of infinitely heavy technifermions [14]. In the considering CSTC scenario, this problem does not appear at all.

The calculations in a more elaborate case with the SM-like technifermion hypercharge $Y_{\tilde{Q}} = 1/3$ are less transparent and more cumbersome. Remarkably enough, in this case $S^{\tilde{\pi}+\tilde{Q}}$ and $U^{\tilde{\pi}+\tilde{Q}}$ are not zeroth any longer but still strongly suppressed. Since in the first, linear, order in q^2 power expansion technipions and technifermions do not contribute or contribute very little, it is worth going beyond this approximation and also incorporating V, W, X parameters into the analysis. Keeping the degeneracy condition $\Delta M_{\tilde{Q}} = 0$, we have $T^{\tilde{\pi}+\tilde{Q}} = 0$, as shown above, and other parameters read

$$S^{\tilde{\pi}+\tilde{Q}} = \frac{2c_W^4}{3\pi}\left\{\frac{1}{3} - \beta_Z^{\tilde{\pi}}(1 - \phi_Z^{\tilde{\pi}}) + N_{\mathrm{TC}}\left(1 + \frac{s_W^4}{9c_W^4}\right)\left[-\frac{1}{3} + (3 + \beta_Z^{\tilde{Q}})(1 - \phi_Z^{\tilde{Q}})\right]\right\},$$

$$U^{\tilde{\pi}+\tilde{Q}} = \frac{2}{3\pi}\left\{\frac{1}{3}(1 - c_W^4) - \beta_W^{\tilde{\pi}}(1 - \phi_W^{\tilde{\pi}}) + c_W^4\beta_Z^{\tilde{\pi}}(1 - \phi_Z^{\tilde{\pi}}) + N_{\mathrm{TC}}\left[-\frac{1}{3}\left(1 - c_W^4 - \frac{1}{9}s_W^4\right) + (3 + \beta_W^{\tilde{Q}})(1 - \phi_W^{\tilde{Q}}) - \left(c_W^4 + \frac{1}{9}s_W^4\right)(3 + \beta_Z^{\tilde{Q}})(1 - \phi_Z^{\tilde{Q}})\right]\right\},$$

$$V^{\tilde{\pi}+\tilde{Q}} = \frac{c_W^2}{6\pi s_W^2}\left\{-\frac{1}{2}M_Z^2\beta_Z^{\tilde{\pi}}B_0'(M_Z^2, m_{\tilde{\pi}}^2, m_{\tilde{\pi}}^2) + (\beta_Z^{\tilde{\pi}} + 1)(1 - \phi_Z^{\tilde{\pi}}) + N_{\mathrm{TC}}\left(1 + \frac{s_W^4}{9c_W^4}\right)\left[\frac{1}{2}M_Z^2(3 + \beta_Z^{\tilde{Q}})B_0'(M_Z^2, M_{\tilde{Q}}^2, M_{\tilde{Q}}^2) - (1 + \beta_Z^{\tilde{Q}})(1 - \phi_Z^{\tilde{Q}})\right]\right\},$$

$$W^{\tilde{\pi}+\tilde{Q}} = \frac{1}{6\pi s_W^2}\left\{-\frac{1}{2}M_W^2\beta_W^{\tilde{\pi}}B_0'(M_W^2, m_{\tilde{\pi}}^2, m_{\tilde{\pi}}^2) + (\beta_W^{\tilde{\pi}} + 1)(1 - \phi_W^{\tilde{\pi}}) + N_{\mathrm{TC}}\left[\frac{1}{2}M_W^2(3 + \beta_W^{\tilde{Q}})B_0'(M_W^2, M_{\tilde{Q}}^2, M_{\tilde{Q}}^2) - (1 + \beta_W^{\tilde{Q}})(1 - \phi_W^{\tilde{Q}})\right]\right\},$$

$$X^{\tilde{\pi}+\tilde{Q}} = \frac{c_W^2}{6\pi}\left\{-\frac{1}{3} + \beta_Z^{\tilde{\pi}}(1 - \phi_Z^{\tilde{\pi}}) + N_{\mathrm{TC}}\left(1 - \frac{s_W^2}{9c_W^2}\right)\left[\frac{1}{3} - (3 + \beta_Z^{\tilde{Q}})(1 - \phi_Z^{\tilde{Q}})\right]\right\},$$

where

$$\beta_{Z,W}^{\tilde{\pi}} = \frac{4m_{\tilde{\pi}}^2}{M_{Z,W}^2} - 1 > 0, \qquad \beta_{Z,W}^{\tilde{Q}} = \frac{4M_{\tilde{Q}}^2}{M_{Z,W}^2} - 1 > 0,$$

$$\phi_{Z,W}^{\tilde{\pi},\tilde{Q}} = (\beta_{Z,W}^{\tilde{\pi},\tilde{Q}})^{1/2}\arctan(\beta_{Z,W}^{\tilde{\pi},\tilde{Q}})^{-1/2},$$

$$B_0'(M^2, m^2, m^2) = \int_0^1 dx\frac{x(1-x)}{m^2 - M^2x(1-x)}.$$

In order to constrain the viability of the CSTC model, let us look at the complete EW precision PT (S, T, U, V, W, X) parameters in the general case, appearing due to both the modifications in the scalar sector and the new states propagating in loops, as well as at their dependence on the physical parameters of the model. These are demonstrated in Figs. 9–12. In particular, we see that the S parameter is always restricted by $|S| < 0.03$ and can even turn to zero for small mixing angles $\sin^2\theta \sim 0.2$, moderate values of $\Delta M_{\tilde{Q}} \sim 5$ GeV, and large values of $M_{\tilde{Q}} \gtrsim 600$ GeV, and this is weakly dependent on $M_{\tilde{\sigma}}$ (see Fig. 9). So, we conclude that in the CSTC there is not such a big issue to satisfy the constraints on the S parameter (3.1): The predictions fit well with $|S^{\text{data}}| \lesssim 0.1$ for the whole physically reasonable parameter space.

Does this fortunate conclusion persist also for other PT parameters? The U parameter is strongly suppressed, too, and never exceeds 0.01 while being rather weakly dependent on all the physical parameters except for the mixing angle; however, it never turns into zero exactly $U \gtrsim 0.002$ (see Fig. 9). Thus, both S and U parameters cannot be used for an efficient constraint of the model parameter space at the current level of data uncertainties (3.1). The same holds true for associated oblique corrections beyond the linear q^2

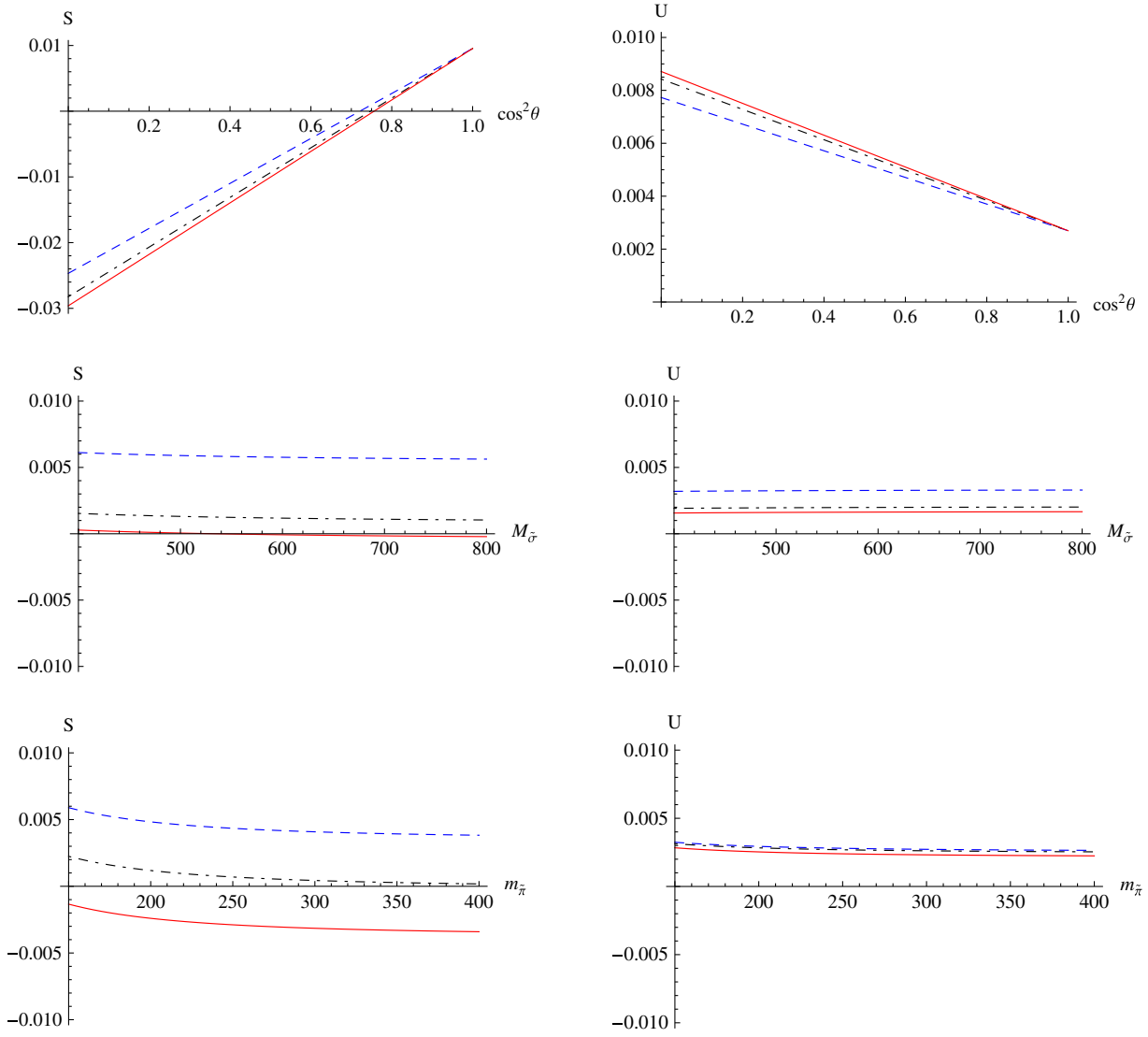

FIG. 9 (color online). The complete S and U parameters in the CSTC scenario (the nonminimal case with μ_S and μ_H included) as functions of (i) $\cos^2\theta$ for fixed $m_{\tilde{\pi}} = 150$ GeV, $M_{\tilde{Q}} \equiv M_U = M_D = 300$ GeV, and $M_{\tilde{\sigma}} = 400$, 600, 800 GeV, corresponding to dashed, dash-dotted, and solid lines, respectively (first row); (ii) $M_{\tilde{\sigma}}$ for fixed $m_{\tilde{\pi}} = 150$ GeV, $\cos^2\theta = 0.9$, and $M_{\tilde{Q}} = 300$, 500, 700 GeV, corresponding to dashed, dash-dotted, and solid lines, respectively (second row); and (iii) $m_{\tilde{\pi}}$ for fixed $M_{\tilde{\sigma}} = 500$ GeV, $\cos^2\theta = 0.9$, $M_{\tilde{Q}} = 300$ GeV, and $\Delta M_{\tilde{Q}} \equiv M_D - M_U = 0$, 5, 10 GeV, corresponding to dashed, dash-dotted, and solid lines, respectively (third row). Also, here and for other PT parameters below, the sine of the mixing angle due to symmetry is chosen to be positive: $s_\theta > 0$.

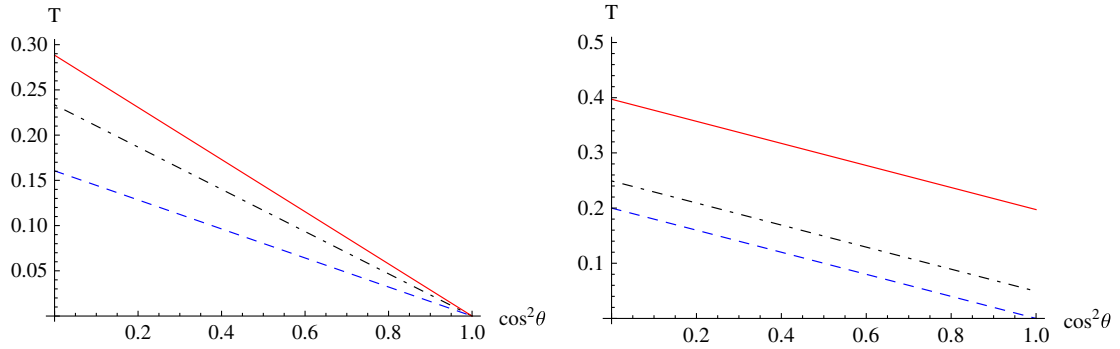

FIG. 10 (color online). The complete T parameter in the CSTC scenario (the nonminimal case with μ_S and μ_H included) as a function of $\cos^2\theta$ for two different cases: (i) $\Delta M_{\tilde{Q}} = 0$ and $M_{\tilde{\sigma}} = 400, 600, 800$ GeV, corresponding to dashed, dash-dotted, and solid lines, respectively (left panel); (ii) $M_{\tilde{\sigma}} = 500$ GeV and $\Delta M_{\tilde{Q}} \equiv M_D - M_U = 0, 5, 10$ GeV, corresponding to dashed, dash-dotted, and solid lines, respectively (right panel). The T parameter does not depend on degenerated $M_{\tilde{Q}} \equiv M_U = M_D$ mass and $m_{\tilde{\pi}}$.

power expansions, given in terms of V, W, X parameters (3.6). In particular, V and W parameters remain of the same order of magnitude as the S and U parameters. They belong to the interval $0.002 \lesssim V,\ W \lesssim 0.01$ and are weakly dependent on physical parameters (see Fig. 11), whereas the X parameter is even more strongly suppressed, $|X| \sim 0.001$ (see Fig. 12). In general, this situation is not noticeably affected by having more than one generation of technifermions or other N_{TC} different from three.

The strongest bounds to the CSTC parameter space actually come from the T parameter (see Fig. 10). The EW precision constraints to the T parameter encoding the vector isospin breaking effects (3.1) are satisfied only for a relatively small $h\tilde{\sigma}$ mixing $\sin^2\theta \lesssim 0.3$ and a small splitting between current technifermion masses $\Delta M_{\tilde{Q}} \lesssim 5$ GeV. The latter is natural, since similarly the relatively small splitting between the current up- and down-quark masses compared to their constituent masses applies also

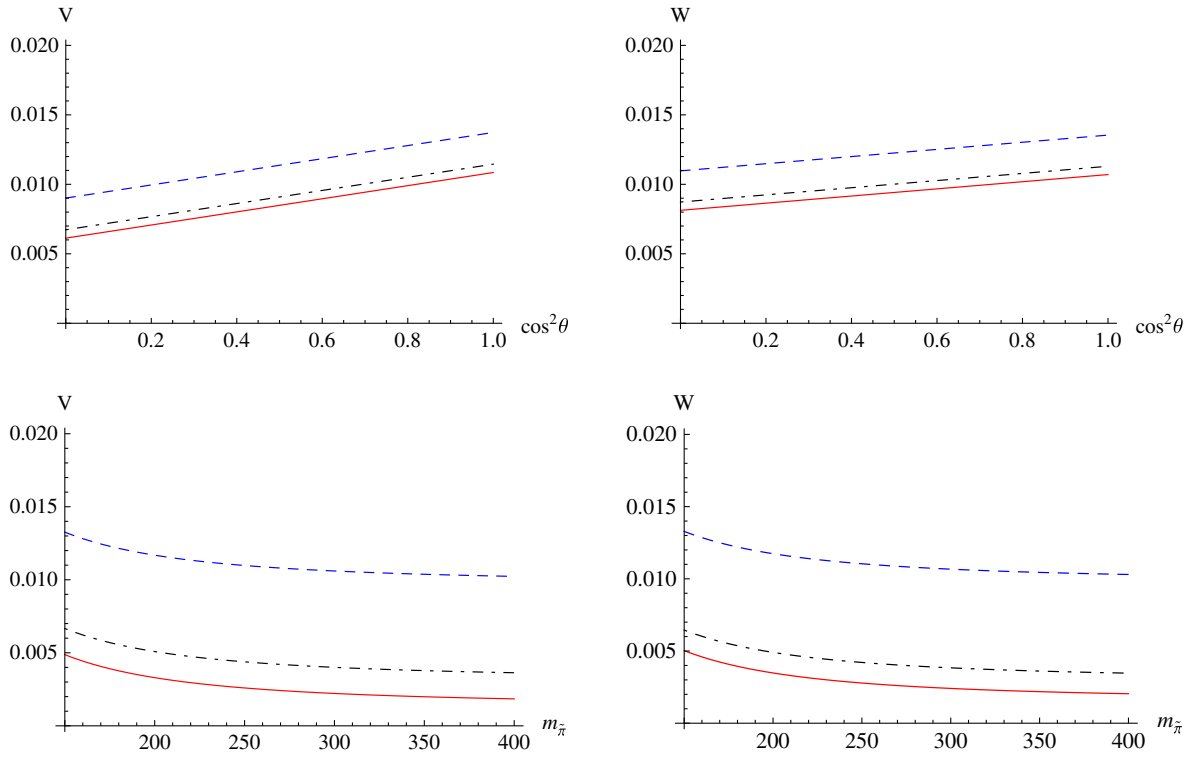

FIG. 11 (color online). The complete V and W parameters in the CSTC scenario (the nonminimal case with μ_S and μ_H included) as functions of (i) $\cos^2\theta$ for fixed $M_U = M_D = 300$ GeV and $m_{\tilde{\pi}} = 150, 250, 350$ GeV, corresponding to dashed, dash-dotted, and solid lines, respectively (first row); and (ii) $m_{\tilde{\pi}}$ for fixed $\cos^2\theta = 0.9$ and $M_{\tilde{Q}} = 300, 500, 700$ GeV, corresponding to dashed, dash-dotted, and solid lines, respectively (second row). Both V and W parameters do not depend on $M_{\tilde{\sigma}}$ and $\Delta M_{\tilde{Q}}$.

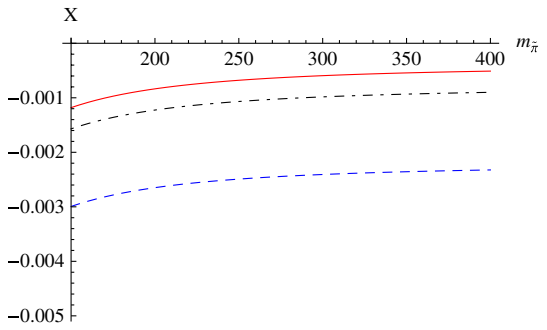

FIG. 12 (color online). The X parameter $m_{\tilde{\pi}}$ for fixed $M_{\tilde{Q}} =$ 300, 500, and 700 GeV, corresponding to dashed, dash-dotted, and solid lines, respectively. It does not depend on $\cos^2\theta$, $M_{\tilde{\sigma}}$, and $\Delta M_{\tilde{Q}}$.

for usual QCD. In the degenerated case with $\Delta M_{\tilde{Q}} = 0$ and in the no $h\tilde{\sigma}$-mixing limit $\cos^2\theta \to 1$, the T parameter vanishes identically: $T \to 0$. So, the CSTC model has enough room to fit with the EW precision data, together with tight constraints to the Higgs sector properties.

Note that the S, U, V, W, X parameters are always UV finite. The T parameter is finite in the degenerated case when $M_U = M_D$, whereas in the general case it has logarithmic divergence proportional to the technifermion mass difference, i.e., $\mathrm{div}(T) \sim (M_U - M_D)^2/\varepsilon$ with a constant coefficient. Note also that the EW constraints put much stronger limits on parameter space in the case of inverse mass hierarchy in the scalar sector of the theory, i.e., assuming that technisigma is the lightest scalar particle observed at the LHC $M_{\tilde{\sigma}} < M_h$. In this case, the $h\tilde{\sigma}$-mixing angle has to be much closer to being vanished in order to satisfy the constraints on the corresponding oblique corrections.

B. Qualitative remarks on FCNC constraints

Another source of (less) stringent constraints onto TC models comes from the FCNC-induced processes (see e.g., Ref. [49]). In particular, here one would be interested in constraints coming from such processes as mixing in the system of neutral mesons $M^0 - \bar{M}^0$, as well as from rare leptonic decays of neutral mesons $M^0 \to l\bar{l}$, etc. The semileptonic decays are presumably more uncertain theoretically due to larger contributions from poorly known hadronic form factors, thus making it rather hard to set definite constraints to NP contributions. The flavor constraints can be very relevant for phenomenological tests of the TC models with relatively light spin-1 resonances with the same quantum numbers as the SM gauge bosons. In the considered CSTC model under discussion adopting the QCD-like mass hierarchy in the technihadron spectrum, there are no light spin-1 particles; heavy vector $\tilde{\rho}$ and axial-vector $\tilde{a}_1$ states are considered to be decoupled from the lightest technipion and technisigma states and do not participate in processes at low momentum transfers. This is, of course, a valid approximation motivated by advances of the usual hadron physics. An extended theory which supposedly includes heavy states should then be quantitatively tested against the flavor constraints according to Ref. [49], in particular, setting up the low bounds on masses of heavy (pseudo)vector particles. However, this analysis will be reasonable only after the lightest (pseudo) scalar states have been discovered experimentally.

In Fig. 13, we illustrate new contributions (besides those in the gauge boson polarizations) to typical FCNC processes (rightmost diagrams), along with the standard part (first two diagrams on the left-hand side). These diagrams describe the short-distance contributions, which dominate the FCNC observables for heavy flavor mesons (for instance, B_d^0 and B_s^0). In the framework of the CSTC model, an additional effect comes only from the $h\tilde{\sigma}$ mixing, whereas technipions and technifermions can contribute only to the gauge boson polarization functions inside the loop propagators.

The qualitative analysis of these contributions reveals that these contributions are strongly suppressed due to the following arguments:

(i) The typical contributions from two-loop FCNC effects with the Higgs boson in the t channel in neutral mesons $M^0 - \bar{M}^0$ mixing are extremely small and usually neglected in the SM calculations. An additional (small) mixing with the heavy $\tilde{\sigma}$ field cannot change this situation noticeably.

(ii) In the case of rare (semi)leptonic decays of the Higgs boson, as well as the $\tilde{\sigma}$ meson, Yukawa couplings to leptons are usually very small ($\sim g m_l/M_W$), and the corresponding contributions are also neglected.

(iii) In all cases the $\tilde{\sigma}$ contributions are additionally suppressed by a large technisigma mass compared to vector boson masses, $M_{\tilde{\sigma}} \gg M_{W,Z}$.

(iv) An extra (double) suppression in the limit of small $h\tilde{\sigma}$ mixing by $s_\theta^2 \ll 1$ factor in the amplitude.

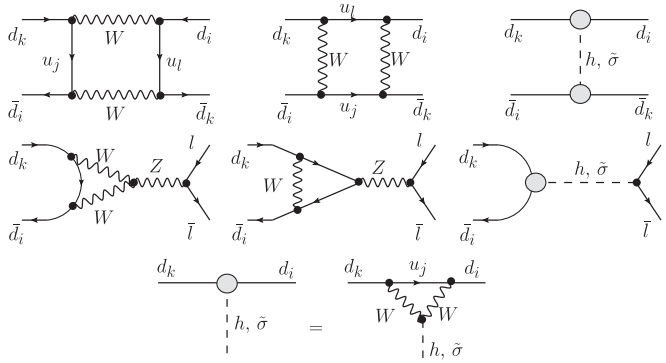

FIG. 13. Typical FCNC contributions in the CSTC model. The rightmost diagrams with scalar exchanges are the only weakly affected contributions due to a small $h\tilde{\sigma}$-mixing and additional $\tilde{\sigma}$ meson, which are however negligibly small (see the main text).

(v) The higher-loop effect from the technipions and technifermions contributing only to the gauge boson polarization functions inside the loop propagators vanishes at small loop momentum $q^2 \to 0$ but otherwise is expected to be extremely small.

We conclude that the most stringent constraints on the parameter space in the considered CSTC scenario come from the T parameter which sets the upper bound to the $h\tilde{\sigma}$ mixing (see previous section). Now, we turn to a discussion of the phenomenological consequences of the CSTC.

IV. COLLIDER PHENOMENOLOGY OF THE CSTC

A. Higgs boson production and decay

The properties of the Higgs sector in the SM are the subject of intensive studies and discussions in light of the latest data from the LHC [1,2,4]. The Higgs couplings are expected to be rather sensitive to NP contributions and could therefore serve as a good probe of physics beyond the SM. However, it is important to notice here that, even though the Higgs boson may look standard according to the latest observations and studies, this does not totally exclude a possible role of NP in the EWSB and, in particular, in its underlined dynamical reasons. Further in this subsection, we will examine basic possible signatures of the CSTC in Higgs boson observables.

Consider first the simplest s-channel subprocess of the Higgs boson production with subsequent decay into final states, i.e., $ab \to h \to XY$. Typically, the initial states of this subprocess are $ab = gg, ZZ, WW$, and the final states are $XY = f\bar{f}, WW^*, ZZ^*, \gamma\gamma$, and γZ. As is seen from the physical Lagrangian of the Higgs boson interactions (2.27) and (2.28), the standard tree-level hVV and $hf\bar{f}$ couplings are modified by a common factor c_θ only caused by a mixing with heavy technisigma state.

For $ab = gg$, the ggh and $gg\tilde{\sigma}$ couplings are loop induced via heavy quarks, and there are no additional loop diagrams can contribute here in the framework of CSTC. Hence, in the Higgs boson production amplitude, there always comes an extra factor c_θ compared to the corresponding SM amplitude. Furthermore, the first three Higgs decay channels $XY = f\bar{f}, WW^*, ZZ^*$ are the tree-level ones, with another factor c_θ in the amplitude, so the corresponding amplitudes $VV \to h \to f\bar{f}, WW^*, ZZ^*$ can only be different with respect to the SM ones by a factor of c_θ^2 only (or a factor of s_θ^2 in the case of the intermediate $\tilde{\sigma}$ meson). But this is true only if one considers the s-channel production process far from the resonance: $\hat{s}^{\rm res} = M_h^2$ (or $\hat{s}^{\rm res} = M_{\tilde{\sigma}}^2$ for the intermediate $\tilde{\sigma}$ meson). However, in the resonance region the modifications of the SM amplitudes can be different from mere mixing factor multiplication.

In order to calculate the s-channel cross section for the scalar Higgs boson (and $\tilde{\sigma}$ meson) production with two-particle final states, one starts from the universal factorized formula which reproduces the well-known narrow-width approximation formula and has been proven to be exact in the framework of the unstable particles model with a smeared mass shell (see e.g., Ref. [50]):

$$\sigma(ab \to h(q), \tilde{\sigma}(q) \to XY) = \frac{16\pi k_{h,\tilde{\sigma}}}{k_a k_b \bar{\lambda}^2(m_a, m_b; q)} \times \frac{\Gamma(h(q), \tilde{\sigma}(q) \to ab)\Gamma(h(q), \tilde{\sigma}(q) \to XY)}{[q^2 - M_{h,\tilde{\sigma}}^2]^2 + [q\Gamma_{h,\tilde{\sigma}}^{\rm tot}(q)]^2}, \quad (4.1)$$

where $q = p_a + p_b$ is the total s-channel 4-momentum, $k_a = 2J_a + 1$ is the number of polarization states, J_a is the spin of particle a (i.e., $k_{h,\tilde{\sigma}} = 1$), and

$$\bar{\lambda}^2(m_a, m_b; q) = 1 - 2\frac{m_a^2 + m_b^2}{q^2} + \frac{(m_a^2 - m_b^2)^2}{q^4} \quad (4.2)$$

is the normalized Källen function. A good estimate of modifications in h, $\tilde{\sigma}$ couplings in the resonance region where $q^2 \simeq M_{h,\tilde{\sigma}}^2$ can thus be obtained from the formula

$$\sigma(ab \to h, \tilde{\sigma} \to XY) \simeq \frac{16\pi}{k_a k_b \bar{\lambda}^2(m_a, m_b; m_{h,\tilde{\sigma}}) M_{h,\tilde{\sigma}}^2} \times {\rm Br}(h, \tilde{\sigma} \to ab) \cdot {\rm Br}(h, \tilde{\sigma} \to XY). \quad (4.3)$$

As was mentioned above, the Higgs couplings to SM fermions and vector bosons in the considered scenario contain an extra c_θ factor compared to the SM ones, so in the resonance region we have for decay widths and branching fractions to a good accuracy

$$\frac{\Gamma_{\rm tot}^{h,{\rm mod}}}{\Gamma_{\rm tot}^{h,{\rm SM}}} \simeq c_\theta^2, \qquad \frac{{\rm Br}^{\rm mod}(h \to XY)}{{\rm Br}^{\rm SM}(h \to XY)} \simeq 1, \qquad XY = f\bar{f}, WW^*, ZZ^*, \quad (4.4)$$

i.e., for all Born-level Higgs or technisigma decays which strongly dominate in the total decay width. This reveals the fact that the Higgs branching ratios, in fact, in the SM and in the considered CSTC scenario are the same. Thus, according to Eq. (4.3), the ratio between the resonant cross sections in the considered model to the SM one is close to unity:

$$\mu_{f\bar{f},ZZ,WW}^{\rm res} = \frac{\sigma^{\rm mod}(VV \to h(q) \to \bar{f}f, ZZ^*, WW^*)}{\sigma^{\rm SM}(VV \to h(q) \to \bar{f}f, ZZ^*, WW^*)} \simeq 1, \quad q^2 \simeq M_h^2, \quad (4.5)$$

which are essentially the Higgs boson signal strengths in respective channels which were measured earlier at the LHC, and no significant deviations from the SM have been found.

In fact, experimentally one never measures events exactly at the resonance peak position $q^2 = M_h^2$, but one rather has a smearing of the resonance by e.g., detector conditions. In this case, a more precise estimation of the Higgs boson signal strength is given by the ratio of the

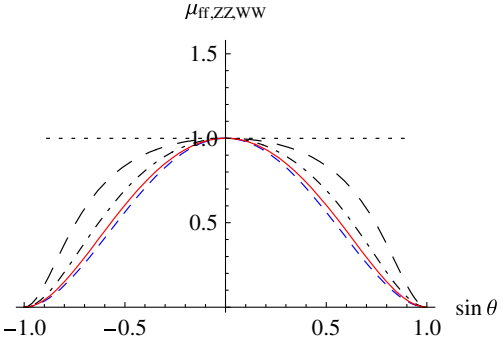

FIG. 14 (color online). The Higgs boson signal strength in the tree-level $f\bar{f}$, ZZ^*, and WW^* channels $\mu_{f\bar{f},WW,ZZ}$ as a function of s_θ calculated according to Eq. (4.6) for $\delta E = 0$ (dotted line), $\delta E = \Gamma^{h,\mathrm{SM}}_{\mathrm{tot}} \simeq 4.03$ MeV (dash-dotted line), $\delta E = \Gamma^{h,\mathrm{SM}}_{\mathrm{tot}}/2$ (long-dashed line), and $\delta E = 2\Gamma^{h,\mathrm{SM}}_{\mathrm{tot}}$ (solid line), and the $c^4_\theta = (1 - s^2_\theta)^2$ curve is also shown for reference (dashed line).

cross sections integrated (or averaged) over the energy resolution of an experiment δE which can be comparable to or exceed the small Higgs boson decay width in the SM, $\delta E \geq \Gamma^{h,\mathrm{SM}}_{\mathrm{tot}} \simeq 4.03$ MeV (at $M_h \simeq 125$ GeV) [11], i.e.,

$$\mu_{\mathrm{XY}}(\delta E) = \frac{\int_{M_h-\delta E}^{M_h+\delta E} \sigma^{\mathrm{mod}}_{\mathrm{XY}}(q)dq}{\int_{M_h-\delta E}^{M_h+\delta E} \sigma^{\mathrm{SM}}_{\mathrm{XY}}(q)dq} \simeq \frac{\Gamma^{\mathrm{mod}}(h \to ab)\Gamma^{\mathrm{mod}}(h \to XY)}{\Gamma^{\mathrm{SM}}(h \to ab)\Gamma^{\mathrm{SM}}(h \to XY)} \times \frac{\int_{M_h-\delta E}^{M_h+\delta E}[(q^2 - M_h^2)^2 + q^2(\Gamma^{h,\mathrm{SM}}_{\mathrm{tot}})^2]dq}{\int_{M_h-\delta E}^{M_h+\delta E}[(q^2 - M_h^2)^2 + q^2(\Gamma^{h,\mathrm{mod}}_{\mathrm{tot}})^2]dq}, \tag{4.6}$$

whose values have to be compared to the measured ones. The last part of the formula above is fulfilled approximately and valid to a good accuracy for $\delta E \gg \Gamma^{h,\mathrm{SM}}_{\mathrm{tot}}$, which is the case in actual measurements. Clearly, the formula (4.6) turns into Eq. (4.5) in the limit of a very narrow δ-shaped resonance, i.e., when $\delta E \ll \Gamma^{h,\mathrm{SM}}_{\mathrm{tot}}$.

In Fig. 14, we show the dependence of the $\mu_{f\bar{f},WW,ZZ}(\delta E)$ on the mixing s_θ for different values of the peak smearing $\delta E = 0$ (short-dashed line), $\delta E = \Gamma^{h,\mathrm{SM}}_{\mathrm{tot}} \simeq 4.03$ MeV (dash-dotted line), and $\delta E = 2\Gamma^{h,\mathrm{SM}}_{\mathrm{tot}}$ (solid line), and the $c^4_\theta = (1 - s^2_\theta)^2$ curve is also shown for reference (dashed line). No smearing case with $\delta E = 0$ corresponds precisely to the resonance formula (4.5) with the unit strength, while an increase in the peak smearing quickly approaches the off-resonance result with $\mu_{f\bar{f},WW,ZZ} \sim c^4_\theta$. Clearly, an influence of the peak smearing vanishes in the no-mixing limit $s_\theta \to 0$.

The near-resonance approximation in the s-channel production process (4.5) is valid up to relatively small loop-induced contributions and higher order correction which may contain extra loop contributions with technipions, technisigma, and technifermions. These extra contributions can be especially pronounced in the loop-induced $\gamma\gamma$ and γZ decay channels (see Fig. 15). Indeed,

$$\mu^{\mathrm{res}}_{\gamma\gamma} = \frac{\sigma^{\mathrm{mod}}(h \to \gamma\gamma)}{\sigma^{\mathrm{SM}}(h \to \gamma\gamma)} \simeq \frac{1}{c^2_\theta}\frac{\Gamma^{\mathrm{mod}}(h \to \gamma\gamma)}{\Gamma^{\mathrm{SM}}(h \to \gamma\gamma)} \simeq \frac{1}{c^2_\theta}\frac{|A_W + A_f + A_{\tilde{\pi}} + A_{\tilde{Q}}|^2}{|A^{\mathrm{SM}}_W + A^{\mathrm{SM}}_f|^2}, \tag{4.7}$$

where $A_{W,f,\tilde{\pi},\tilde{Q}}$ are the amplitudes given by the SM-like W, f loop diagrams [see Figs. 15(a)–15(c)], as well as by the new technipion $\tilde{\pi}$ and technifermion $\tilde{Q}$ loop diagrams [see Figs. 15(c)–15(e)]. An interference effect between these contributions may be important. Notably, $A_{\tilde{Q}} \sim s_\theta$ while $|A_{\tilde{\pi}}| \ll |A_{\tilde{Q}}|$ in general, so the interference effect changes its sign depending on the sign of s_θ possibly giving rise to either enhancement or suppression of the $\gamma\gamma$ signal or to the SM-like $h \to \gamma\gamma$ signal strengths in the case of a small mixing angle $s_\theta \ll 1$ (where the technipion loop contribution disappears as well). Since the first three diagrams, which are present in the SM, do not exist at the tree level, their sum is free of divergencies. More precisely, the divergencies are canceled between diagrams (a) and (b),

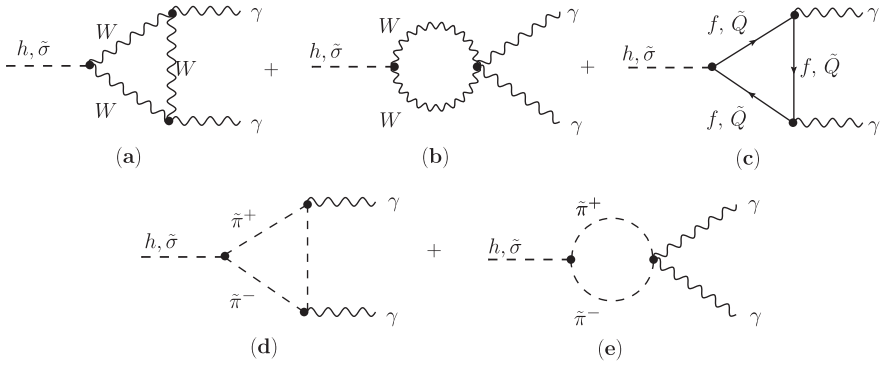

FIG. 15. Typical one-loop contributions to the $h, \tilde{\sigma} \to \gamma\gamma$ decay channel in the CSTC.

and the fermion (f and $\tilde{Q}$) loops are finite individually. We have found that the sum of technipion loops is finite as well. Also, here it is reasonable to assume that only heavy top-quark loops contribute to the final result; all other fermions are strongly suppressed and thus can be neglected.

A straightforward calculation leads to the following Higgs partial decay width in the $\gamma\gamma$ channel:

$$\Gamma^{\mathrm{mod}}(h\to\gamma\gamma)=\frac{\alpha^2 M_h}{16\pi^3}\cdot|F_W+F_{\mathrm{top}}+F_{\tilde{\pi}}+F_{\tilde{Q}}|^2, \tag{4.8}$$

where $\alpha=\alpha(M_Z)=1/127.93$ is the fine structure constant adopted in all numerical calculations, and the individual contributions from W, top-quark, $\tilde{\pi}$, and $\tilde{Q}$ loops read, respectively,

$$\begin{aligned}
F_W &= \frac{1}{8} g c_\theta \frac{M_h}{M_W}\cdot[2+3\beta_W+3\beta_W(2-\beta_W)f(\beta_W)],\\
F_{\mathrm{top}} &= -\frac{4}{3} g c_\theta \frac{m_{\mathrm{top}}^2}{M_h M_W}[1+(1-\beta_{\mathrm{top}})f(\beta_{\mathrm{top}})],\\
F_{\tilde{\pi}} &= -\frac{g_{h\tilde{\pi}}}{2M_h}[1-\beta_{\tilde{\pi}}f(\beta_{\tilde{\pi}})],\\
g_{h\tilde{\pi}} &= -2(\lambda_{\mathrm{TC}} u s_\theta - \lambda v c_\theta),\\
F_{\tilde{Q}} &= -2N_{\mathrm{TC}}(q_U^2+q_D^2) g_{\mathrm{TC}} s_\theta \frac{M_{\tilde{Q}}}{M_h}[1+(1-\beta_{\tilde{Q}})f(\beta_{\tilde{Q}})],
\end{aligned} \tag{4.9}$$

where we take the number of technicolors $N_{\mathrm{TC}}=3$ in numerical calculations below, $q_{U,D}$ are the techni-up and techni-down fermion charges, and

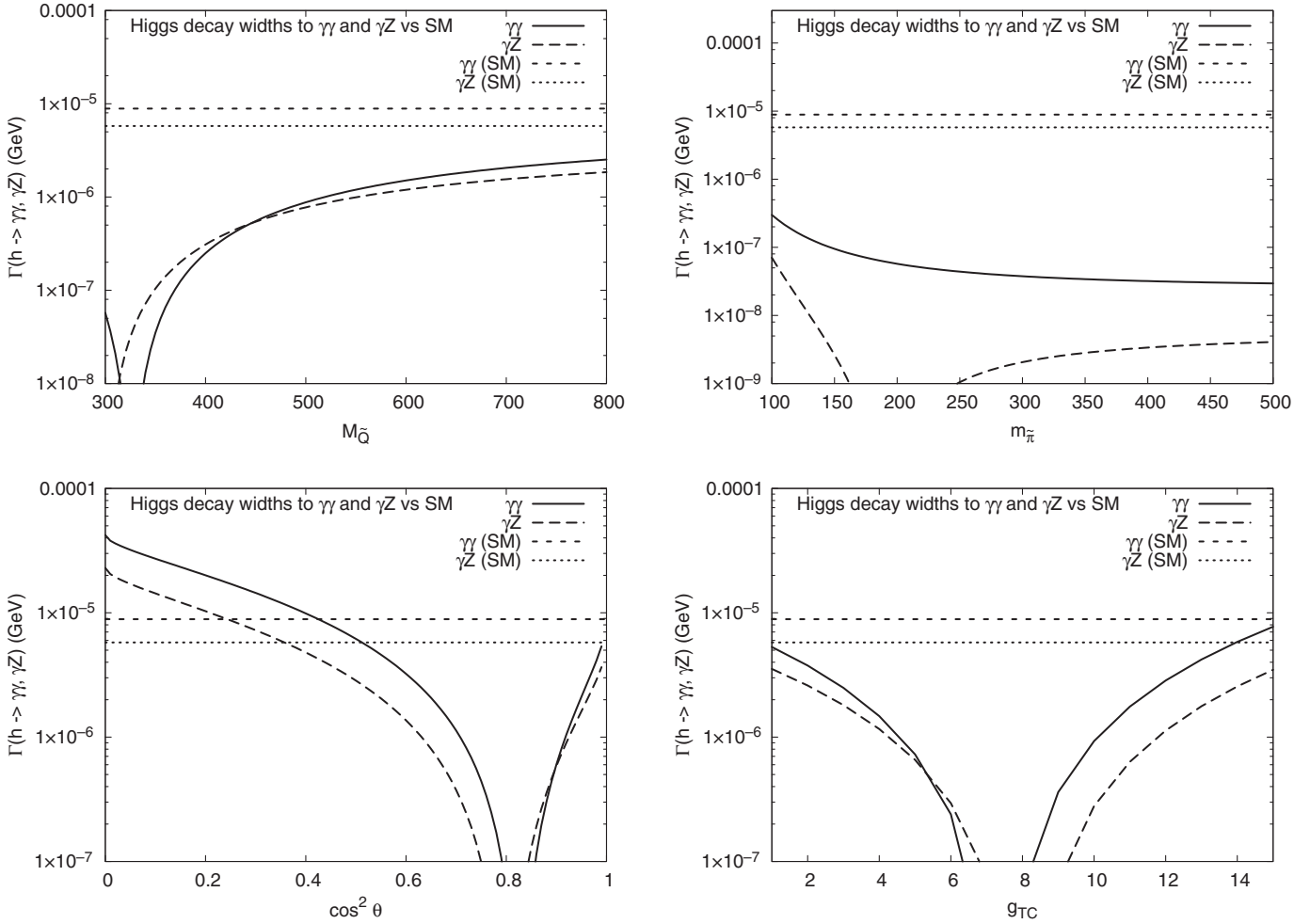

FIG. 16. The Higgs boson decay widths in the loop-induced $\gamma\gamma$ and γZ channels in the nonminimal CSTC (with scalar $\mu_{S,H}$ terms included) as functions of physical parameters of the model. The corresponding SM predictions are shown for comparison. The parameters in each figure are set as follows: (top left) $m_{\tilde{\pi}}=200$ GeV, $c_\theta^2=0.8$, and $g_{\mathrm{TC}}=8$; (top left) $M_{\tilde{Q}}=300$ GeV, $c_\theta^2=0.8$, and $g_{\mathrm{TC}}=8$; (bottom left) $M_{\tilde{Q}}=300$ GeV, $m_{\tilde{\pi}}=200$ GeV, and $g_{\mathrm{TC}}=8$; (bottom right) $M_{\tilde{Q}}=300$ GeV, $m_{\tilde{\pi}}=200$ GeV, and $c_\theta^2=0.8$. These results do not depend on $M_{\tilde{\sigma}}$, and the positive sign of the mixing angle, or $s_\theta>0$, is fixed here.

$$f(\beta) = \arcsin^2 \frac{1}{\sqrt{\beta}} \qquad \beta_X = \frac{4m_X^2}{M_h^2}, \qquad X = W, \text{top}, \tilde{\pi}, \tilde{Q}. \tag{4.10}$$

In the nonminimal case with scalar μ terms included, the relation

$$g_{h\tilde{\pi}} = -g_{\rm TC} s_\theta \frac{M_h^2 - m_{\tilde{\pi}}^2}{M_{\tilde{Q}}} \tag{4.11}$$

can be used [cf. Eq. (2.28)], whereas in the special case with $\mu_{S,\rm H} \to 0$ the relations (2.37) have to be employed for calculation of the $g_{h\tilde{\pi}}$ coupling. In the limit of small $h\tilde{\sigma}$ mixing, the constituent technifermion and technipion loop contributions to the Higgs boson width are suppressed by a factor of $s_\theta^2 \ll 1$, so the whole expression (4.8) turns to the SM result:

$$\Gamma^{\rm SM}(h \to \gamma\gamma) = \frac{\alpha^2 M_h}{16\pi^3} \cdot |F_W^{\rm SM} + F_{\rm top}^{\rm SM}|^2, \tag{4.12}$$

where $F_{W,\rm top}^{\rm SM}$ can be obtained from Eq. (4.9) with $c_\theta = 1$.

The Higgs boson decay widths in the loop-induced $\gamma\gamma$ and also in the γZ channels in the nonminimal CSTC with scalar $\mu_{S,H}$ terms included are shown in Fig. 16 as functions of physical parameters of the model. This figure covers only the $s_\theta > 0$ region and is complementary to Fig. 18. One notices the regions where the $\gamma\gamma$ and γZ widths can be very different from the SM predictions, or close to them, or even turn to zero due to a specific interference pattern. Also, the relation between $\gamma\gamma$ and γZ widths strongly depends on parameters. It is, however, more instructive to look directly at the Higgs signal strengths in the respective decay channels as functions of parameters, and we will primarily study the $\gamma\gamma$ channel in detail here.

In particular, let us investigate to what extent the $h\tilde{\sigma}$ mixing and the presence of the extra new $\tilde{\pi}$ and $\tilde{Q}$ states in loops affects the resonance Higgs signal strength in the $\gamma\gamma$ channel $\mu_{\gamma\gamma}^{\rm res}$ and its smearing, given by Eqs. (4.7) and (4.6), respectively. For this purpose, in Fig. 17, we show the Higgs boson signal strength in the $\gamma\gamma$ channel in the resonance region $\mu_{\gamma\gamma}^{\rm res}(s_\theta)$ given by Eq. (4.7) in the nonminimal case of the CSTC model with scalar $\mu_{S,H}$ terms included. The $\mu_{\gamma\gamma}^{\rm res}(s_\theta)$ weakly depends on the $m_{\tilde{\pi}}$ value. It also turns into zero at some $s_\theta^* > 0$, which increases with $M_{\tilde{Q}}$ and decreases with $g_{\rm TC}$. Note that there is no symmetry $s_\theta \to -s_\theta$. In general, for $s_\theta < 0$, we always have in the resonance $\mu_{\gamma\gamma}^{\rm res}(s_\theta) > 1$, while smearing over the resonance can change this. Also, smearing does not change significantly $\mu_{\gamma\gamma}^{\rm res}(s_\theta)$ at small smearing angles $s_\theta \to 0$.

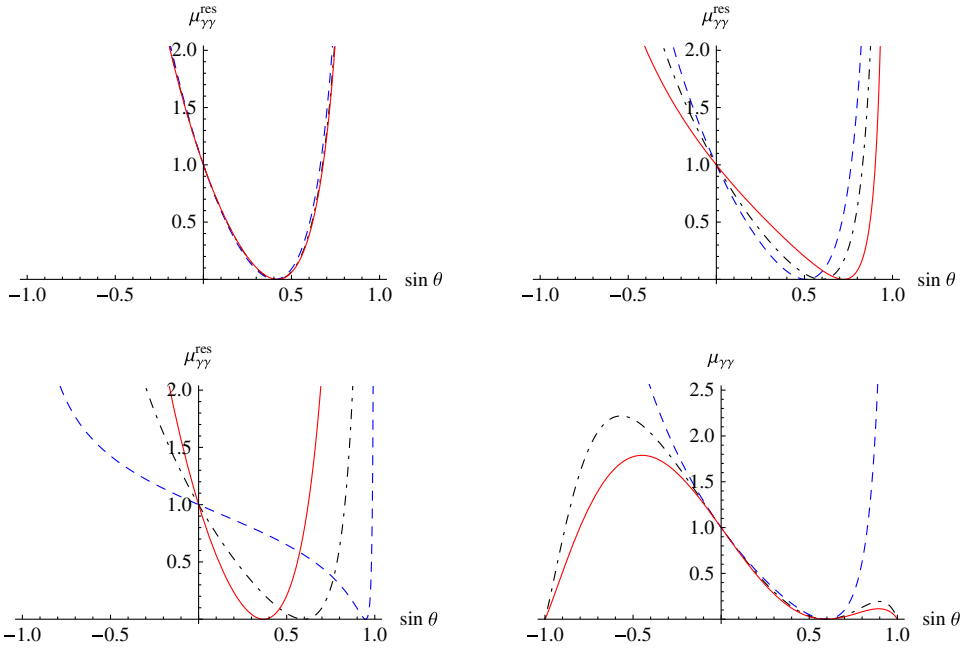

FIG. 17 (color online). Dependence of the Higgs boson signal strength in the resonance given by Eq. (4.7) in the nonminimal case of the CSTC model (with scalar $\mu_{S,H}$ terms included), $\mu_{\gamma\gamma}^{\rm res}$, on s_θ for different sets of the physical parameters: (top left) $g_{\rm TC} = 8$, $M_{\tilde{Q}} = 300$ GeV, and $m_{\tilde{\pi}} = 150, 250, 350$ GeV, corresponding to dashed, dash-dotted, and solid lines, respectively; (top right) $g_{\rm TC} = 8$, $m_{\tilde{\pi}} = 150$ GeV, and $M_{\tilde{Q}} = 400, 500, 700$ GeV, corresponding to dashed, dash-dotted, and solid lines, respectively; (bottom left) $m_{\tilde{\pi}} = 150$ GeV, $M_{\tilde{Q}} = 500$ GeV, and $g_{\rm TC} = 2, 8, 15$, corresponding to dashed, dash-dotted, and solid lines, respectively. Finally, the bottom-right figure corresponds to smeared $\mu_{\gamma\gamma}(\delta E)$ given by Eq. (4.6) as a function of s_θ for fixed $m_{\tilde{\pi}} = 150$ GeV, $M_{\tilde{Q}} = 500$ GeV, and $g_{\rm TC} = 8$ and with different smearing parameters: no smearing $\delta E = 0$ (dashed line), $\delta E = \Gamma_{\rm tot}^{h,\rm SM} \simeq 4.03$ MeV (dash-dotted line), and $\delta E = 1$ GeV (solid line). Here and below, $Y_{\tilde{Q}} = 1/3$, unless noted otherwise.

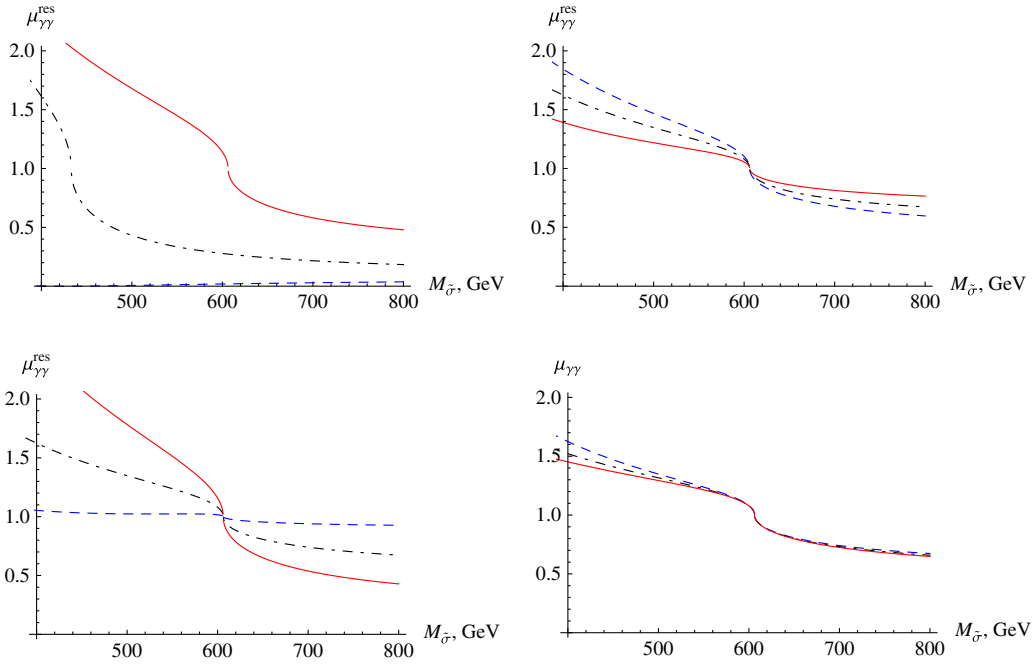

FIG. 18 (color online). Dependence of the Higgs boson signal strength in the resonance given by Eq. (4.7) in the minimal CSTC model (with scalar $\mu_{S,H}$ terms excluded), $\mu^{\rm res}_{\gamma\gamma}$, on $M_{\tilde\sigma}$ for different sets of the physical parameters: (top left) $g_{\rm TC} = 8$, $M_{\tilde Q} = 300$ GeV, and $m_{\tilde\pi} = 150, 250, 350$ GeV, corresponding to dashed, dash-dotted, and solid lines, respectively; (top right) $g_{\rm TC} = 8$, $m_{\tilde\pi} = 350$ GeV, and $M_{\tilde Q} = 400, 500, 700$ GeV, corresponding to dashed, dash-dotted, and solid lines, respectively; (bottom left) $m_{\tilde\pi} = 350$ GeV, $M_{\tilde Q} = 500$ GeV, and $g_{\rm TC} = 2, 8, 15$, corresponding to dashed, dash-dotted, and solid lines, respectively. Finally, the bottom-right figure corresponds to smeared $\mu_{\gamma\gamma}(\delta E)$ given by Eq. (4.6) as a function of $M_{\tilde\sigma}$ for fixed $m_{\tilde\pi} = 350$ GeV, $M_{\tilde Q} = 500$ GeV, and $g_{\rm TC} = 8$ and with different smearing parameters: no smearing $\delta E = 0$ (dashed line), $\delta E = \Gamma^{h,\rm SM}_{\rm tot} \simeq 4.03$ MeV (dash-dotted line), and $\delta E = 1$ GeV (solid line).

The signal strength is close to unity for two different cases of the mixing angle: in the no $h\tilde\sigma$-mixing limit $s_\theta \to 0$ and for $s_\theta \sim 0.5$–0.7, while the latter is much more fine-tuned due to a sharp behavior of $\mu^{\rm res}_{\gamma\gamma}(s_\theta)$; the third configuration at negative s_θ appears due to a resonance smearing described above. Note that any relatively large mixing configurations with $s^2_\theta > 0.4$ are excluded by EW precision constraints on the T parameter (see above).

In Fig. 18, we show the same observable $\mu^{\rm res}_{\gamma\gamma}$, but in the minimal CSTC scenario without $\mu_{S,H}$ terms, as a function of $M_{\tilde\sigma}$. In opposition to the nonminimal CSTC, in this case there is a very strong dependence on the $m_{\tilde\pi}$ parameter. Also, in the no-mixing limit $s_\theta \to 0$, which corresponds to $M_{\tilde\sigma} \to \sqrt{3} m_{\tilde\pi}$, the strength turns to unity $\mu^{\rm res}_{\gamma\gamma} \to 1$, as expected, and smearing does not affect this. The current LHC data, in fact, $m_{\tilde\pi} \gtrsim 250$ GeV and the small $h\tilde\sigma$-mixing configuration in the parameter space, and a small vicinity around the no $h\tilde\sigma$-mixing limit is the only region of parameter space which satisfies the data in the minimal CSTC and the Higgs boson looks as the standard one.

At last, in Fig. 19, we show partial contributions to the Higgs signal strength in the resonance $\mu^{\rm res}_{\gamma\gamma}$ coming from the W loop (dashed lines), top-quark loop $\times$ 10 (dash-dotted lines), technifermion loop $\times$ 10 (dotted lines), and technipion loop $\times$ 1000 (short-dashed lines), where the rescalings of the curves are made to increase visibility. The shapes of the curves in the minimal and nonminimal CSTC scenarios are very different, but in both cases there is a strong interference pattern.

B. Technipion and technisigma phenomenology

1. Technipion decay

Besides the Higgs boson decay properties studied above, another important phenomenological implication of the CSTC scenario concerns possible technipion and technisigma signatures at the LHC. Since technipions are pseudoscalar particles, at tree level they can be produced only in pairs $\tilde\pi^+\tilde\pi^-$ or $\tilde\pi^0\tilde\pi^0$, which have rather high invariant masses $M_{\tilde\pi\,\tilde\pi} \gtrsim 300$ GeV, whereas one-technipion production can be loop induced only (see below). In order to define the phenomenological signatures of technisigma and technipion production at colliders, one has to study primarily the decay modes of produced technipions. In particular, an identification of the produced $\tilde\pi$ mesons is important for e.g., studies of the $\tilde\sigma$ meson properties at the LHC, Yukawa and gauge couplings, as well as constituent masses and degeneration of the mass spectrum of the technifermions, etc.

It is of special interest for collider phenomenology to study $\tilde\pi$ decays into vector bosons and, in principle, into a

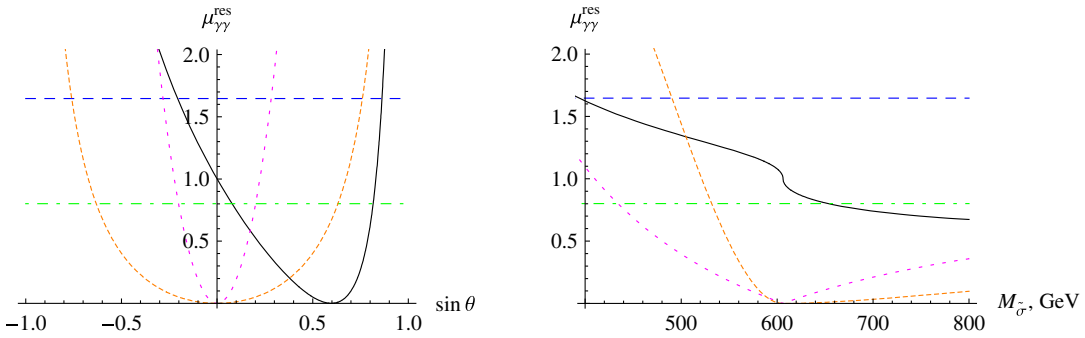

FIG. 19 (color online). Partial contributions to the $\mu_{\gamma\gamma}^{\rm res}$ in the nonminimal CSTC (with scalar $\mu_{S,H}$ terms included) as functions of s_θ with $m_{\tilde{\pi}} = 150$ GeV, $M_{\tilde{Q}} = 500$ GeV, and $g_{\rm TC} = 8$ (left panel) and in the minimal CSTC without scalar $\mu_{S,H}$ terms as functions of $M_{\tilde{\sigma}}$ with $m_{\tilde{\pi}} = 350$ GeV, $M_{\tilde{Q}} = 500$ GeV, and $g_{\rm TC} = 8$ (right panel), corresponding to the W loop (dashed lines), top-quark loop $\times$ 10 (dash-dotted lines), technifermion loop $\times$ 10 (dotted lines), and technipion loop $\times$ 1000 (short-dashed lines). In both panels, solid lines correspond to the total Higgs boson signal (resonant) strengths shown for comparison. The rescaling of the curves is made for better visibility and comparison.

pair Higgs bosons whose diagrams are represented as generic two- and three-body technifermion loop-induced processes in Fig. 20. In the case of the mass-degenerated technifermion doublet, it turns out that in the simplest case with $Y_{\tilde{Q}} = 0$ the two-body technipion vector boson decay modes are always forbidden by symmetry encoded in the structure of vertices, whereas allowed for generic $Y_{\tilde{Q}} \neq 0$ cases. The $\tilde{\sigma}$ decays would manifest themselves as multilepton final states with a large lepton multiplicity—up to 12 leptons from technipion pair decay in the case of $Y_{\tilde{Q}} = 0$ or up to eight leptons for $Y_{\tilde{Q}} = 1/3$ in the final state from technisigma decay (six and four leptons coming from each technipion in the above cases, respectively), which would be rather challenging but very interesting to study.

In general, one would deal with many possible four-vector $VVVV$, four-Higgs $hhhh$, or mixed $hhVV$ final states in order to reconstruct the technisigma mass, and this procedure gets even more complicated due a very large $\tilde{\sigma}$ width. If there are no visible deviations of the Higgs boson properties from the SM ones, the technipion and technisigma phenomenology, as well as Higgs-scalar self-couplings and studies of various loop-induced processes with the Higgs boson participation, even though very challenging, would be the only source of information about the CSTC sector possibly available at the LHC. The technipion two-body decay modes into the on-shell gauge bosons, namely, into the $\gamma\gamma$, γZ, γW, ZZ, and ZW final states (above the corresponding thresholds), in the case with $Y_{\tilde{Q}} = 1/3$ are given by

$$\Gamma(\tilde{\pi}^0 \to \gamma\gamma) = \frac{\alpha^2 g_{\rm TC}^2}{4\pi^3}\frac{M_{\tilde{Q}}^2}{m_{\tilde{\pi}}}\arcsin^4\left(\frac{m_{\tilde{\pi}}}{2M_{\tilde{Q}}}\right), \qquad \frac{m_{\tilde{\pi}}}{2M_{\tilde{Q}}} < 1,$$

$$\Gamma(\tilde{\pi}^0 \to \gamma Z) = \frac{\alpha^2 g_{\rm TC}^2}{2\pi^3}\frac{M_{\tilde{Q}}^2}{m_{\tilde{\pi}}}\cot^2 2\theta_W\left(1 - \frac{M_Z^2}{m_{\tilde{\pi}}^2}\right) \times \left[\arcsin^2\left(\frac{m_{\tilde{\pi}}}{2M_{\tilde{Q}}}\right) - \arcsin^2\left(\frac{M_Z}{2M_{\tilde{Q}}}\right)\right]^2,$$

$$\Gamma(\tilde{\pi}^\pm \to \gamma W^\pm) = \frac{\alpha^2 g_{\rm TC}^2}{2\pi^3 s_W^2}\frac{M_{\tilde{Q}}^2}{m_{\tilde{\pi}}}\left(1 - \frac{M_W^2}{m_{\tilde{\pi}}^2}\right) \times \left[\arcsin^2\left(\frac{m_{\tilde{\pi}}}{2M_{\tilde{Q}}}\right) - \arcsin^2\left(\frac{M_W}{2M_{\tilde{Q}}}\right)\right]^2,$$

$$\Gamma(\tilde{\pi}^0 \to ZZ) = \frac{\alpha^2 g_{\rm TC}^2}{16\pi^3}M_{\tilde{Q}}^2 m_{\tilde{\pi}}^3 \bar{\lambda}^3(M_Z^2, M_Z^2, m_{\tilde{\pi}}^2) \times C_0^2(M_Z^2, M_Z^2, m_{\tilde{\pi}}^2; M_{\tilde{Q}}^2),$$

$$\Gamma(\tilde{\pi}^\pm \to ZW^\pm) = \frac{\alpha^2 g_{\rm TC}^2}{32\pi^3 c_W^2}M_{\tilde{Q}}^2 m_{\tilde{\pi}}^3 \bar{\lambda}^3(M_Z^2, M_W^2, m_{\tilde{\pi}}^2) \times C_0^2(M_Z^2, M_W^2, m_{\tilde{\pi}}^2; M_{\tilde{Q}}^2),$$

respectively, where the normalized Källen function is defined in Eq. (4.2) and $C_0(m_1^2, m_2^2, m_3^2; m^2) \equiv C_0(m_1^2, m_2^2, m_3^2; m^2, m^2, m^2)$ is the standard finite three-point function. Note that the $\tilde{\pi}^0 \to WW$ decay mode is forbidden by symmetry. The complete set of $\tilde{\pi}$ decay rates (the $\tilde{\pi}^0 \to hh$ decay rate which, in principle, exists for heavy technipions vanishes in the no $h\sigma$-mixing limit

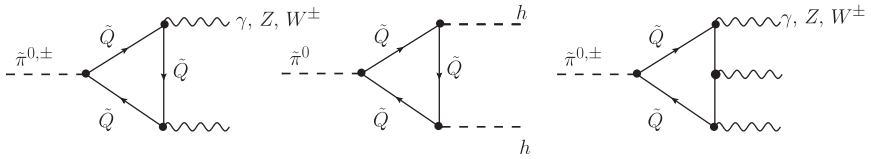

FIG. 20. Light technipion loop-induced (two- and three-body) decay modes in the leading order through constituent technifermion loops.

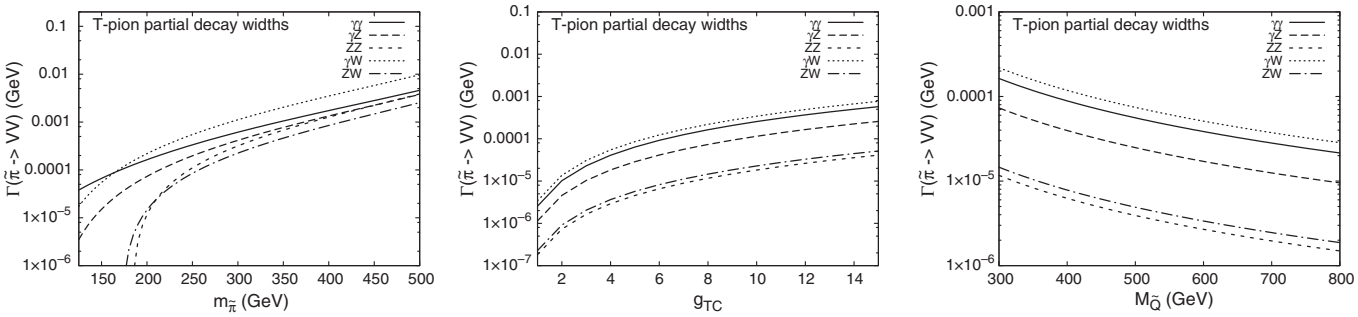

FIG. 21. The technipion decay widths in the loop-induced $\gamma\gamma$, γZ, γW, ZZ, and ZW channels in the nonminimal CSTC (with scalar $\mu_{S,H}$ terms included) as functions of physical parameters of the model. The parameters in each figure are set as follows: (left) $M_{\tilde{Q}} = 300$ GeV, $c_\theta^2 = 0.8$, and $g_{\rm TC} = 8$; (middle) $M_{\tilde{Q}} = 300$ GeV, $m_{\tilde{\pi}} = 200$ GeV, and $c_\theta^2 = 0.8$; (right) $m_{\tilde{\pi}} = 200$ GeV, $c_\theta^2 = 0.8$, and $g_{\rm TC} = 8$. These results do not depend on $M_{\tilde{\sigma}}$.

and is not included into the analysis) is shown for the nonminimal CSTC scenario in Fig. 21 as functions of the model parameters. The branching ratios as functions of $m_{\tilde{\pi}}$ at a fixed point in the parameter space as an example are shown in Fig. 22. Interestingly enough, the total technipion decay width is dominated by the $\gamma W^\pm$ channel in the $\tilde{\pi}^\pm$ decay, and by the $\gamma\gamma$ channel in the $\tilde{\pi}^0$ decay, although other decay modes are not negligible in general.

2. Technisigma decay

The tree-level two-body $\tilde{\sigma}$ decay widths into $\tilde{\pi}\,\tilde{\pi}$, $f\bar{f}$, ZZ, and WW are given by the following expressions:

$$\Gamma(\tilde{\sigma} \to \tilde{\pi}\,\tilde{\pi}) = \frac{3 g^2_{\tilde{\sigma}\,\tilde{\pi}}}{8\pi M_{\tilde{\sigma}}} \sqrt{1 - \frac{4m^2_{\tilde{\pi}}}{M^2_{\tilde{\sigma}}}},$$

$$g_{\tilde{\sigma}\,\tilde{\pi}} = -\lambda_{\rm TC} u c_\theta - \lambda v s_\theta,$$

$$\Gamma(\tilde{\sigma} \to \bar{f} f) = \frac{g^2 s^2_\theta}{32\pi} M_{\tilde{\sigma}} \frac{M^2_f}{M^2_W} \left(1 - \frac{4M^2_f}{M^2_{\tilde{\sigma}}}\right)^{3/2},$$

$$\Gamma(\tilde{\sigma} \to ZZ) = \frac{g^2 s^2_\theta}{16\pi} \frac{M^2_Z}{M_{\tilde{\sigma}} c^2_W} \left(1 - \frac{4M^2_Z}{M^2_{\tilde{\sigma}}}\right)^{1/2} \cdot \left[1 + \frac{(M^2_{\tilde{\sigma}} - 2M^2_Z)^2}{8M^4_Z}\right],$$

$$\Gamma(\tilde{\sigma} \to WW) = \frac{g^2 s^2_\theta}{8\pi} \frac{M^2_W}{M_{\tilde{\sigma}}} \left(1 - \frac{4M^2_W}{M^2_{\tilde{\sigma}}}\right)^{1/2} \cdot \left[1 + \frac{(M^2_{\tilde{\sigma}} - 2M^2_W)^2}{8M^4_W}\right],$$

respectively, while the loop-induced $\tilde{\sigma}$ decay widths in the $\gamma\gamma$ and γZ channels can be obtained from that of the Higgs boson by a replacement $c_\theta \to s_\theta$, $M_h \to M_{\tilde{\sigma}}$, and thus are not shown here explicitly. The (pseudo)scalar (hh and $\tilde{\pi}\,\tilde{\pi}$) decay modes are shown for the nonminimal CSTC scenario in Fig. 23 as functions of the model parameters, while fermion ($t\bar{t}$ and $b\bar{b}$) and gauge boson ($\gamma\gamma$, γZ, ZZ, and WW) decay channels are given in Fig. 24. One notices that the technipion modes of the $\tilde{\sigma}$ decay strongly dominate the total $\tilde{\sigma}$ decay width and can be as large as a few hundred GeV being comparable to $M_{\tilde{\sigma}}$. Certainly, $\tilde{\sigma}$ is a highly unstable and unusually broad state, for which one cannot use the narrow width approximation, and it is an open question how to identify it experimentally.

3. One-technipion production

As has been mentioned above, one technipion can be produced only at the loop level. Let us look into this possibility in more detail, since this channel is especially important for understanding the discovery potential of technicolor at the LHC, even in the absence of any deviations of the Higgs boson signal strengths from the SM predictions. The corresponding typical partonic $2 \to 3$ hard subprocess of Higgs boson and $\tilde{\pi}$ production in high-energy hadron-hadron collisions via the intermediate vector boson fusion (VBF) mechanism is shown in Fig. 25. The Higgs boson VBF production channel (left panel) shown for comparison with the technipion channel (right panel) is one of the key production modes recently studied at the LHC which allowed for clear discrimination of the

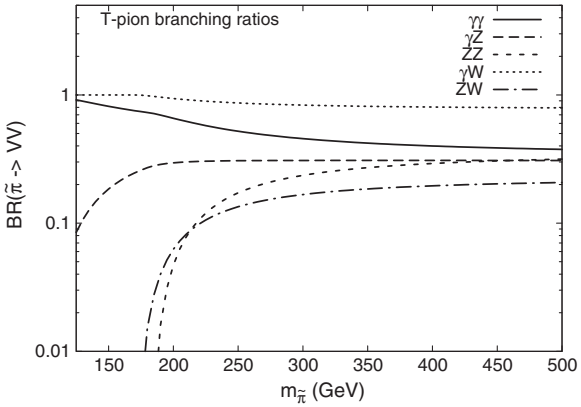

FIG. 22. The neutral and charged technipion branching ratios of the loop-induced $\gamma\gamma$, γZ, γW, ZZ, and ZW channels in the nonminimal CSTC (with scalar $\mu_{S,H}$ terms included) as functions of $m_{\tilde{\pi}}$ for fixed $M_{\tilde{Q}} = 300$ GeV, $c_\theta^2 = 0.8$, and $g_{\rm TC} = 8$.

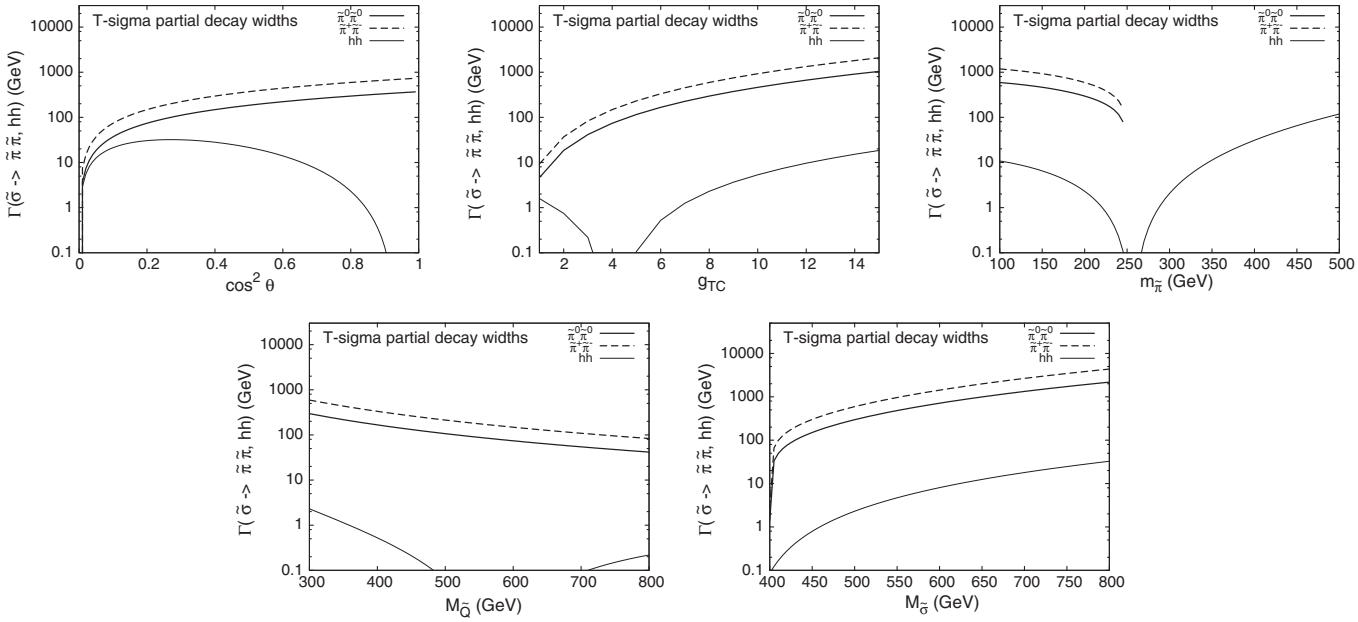

FIG. 23. The technisigma tree-level decay widths in the $\tilde{\pi}\,\tilde{\pi}$ and hh channels in the nonminimal CSTC (with scalar $\mu_{S,H}$ terms included) as functions of physical parameters of the model. The parameters in each figure are fixed as $m_{\tilde{\pi}} = 200$ GeV, $M_{\tilde{Q}} = 300$ GeV, $M_{\tilde{\sigma}} = 500$ GeV, $c_\theta^2 = 0.8$, and $g_{\mathrm{TC}} = 8$, such that in each figure one drops off a variable from this list corresponding to the one at the respective x axis while keeping the others fixed.

Higgs signal and large backgrounds [1,2]. The Higgs boson has also other production modes, e.g., via the gluon-gluon fusion mechanism and the Higgsstrahlung off gauge bosons and heavy flavor. Opposite to the Higgs boson, one technipion can be produced only via a heavy technifermion triangle loop in the VBF mechanism. In numerical estimations, it is explicitly assumed that the incoming quark q and (anti)quark q' lose only a small fraction of their initial energy taken away by intermediate vector bosons. In this kinematics, the final-state quarks are seen as forward-backward hard jets, and by measuring their momenta one accurately reconstructs the invariant mass

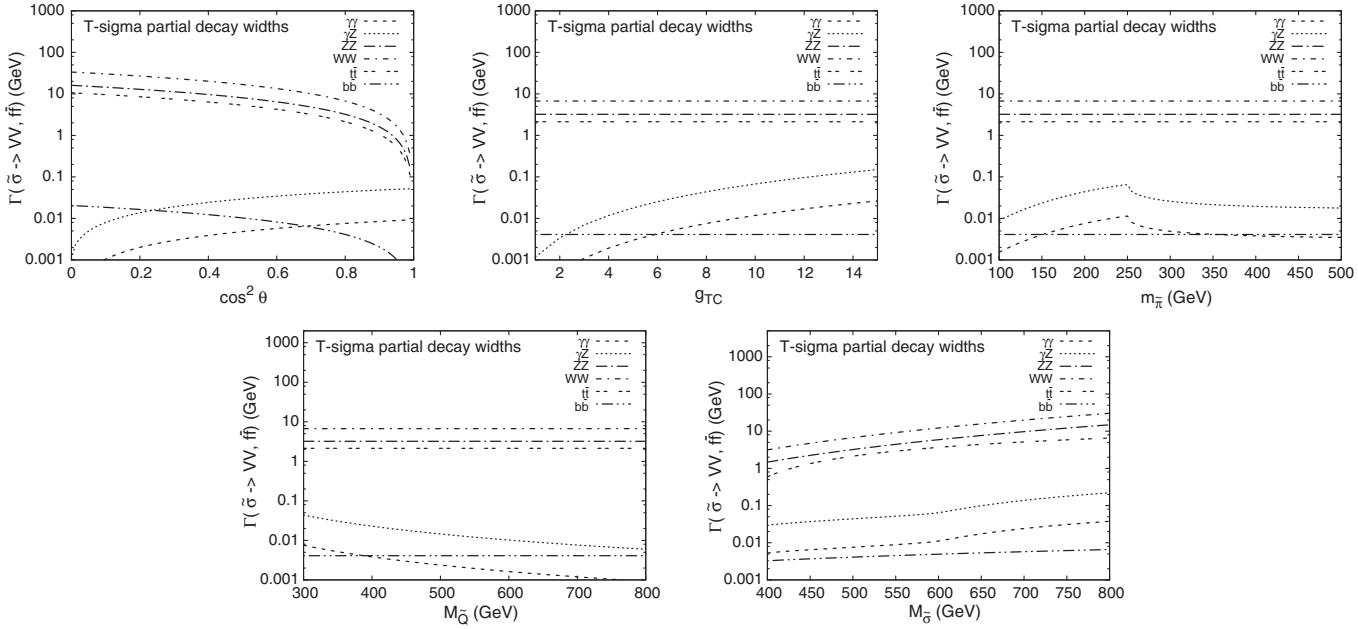

FIG. 24. The technisigma tree-level decay widths in the fermion ($t\bar{t}$ and $b\bar{b}$) and gauge boson ($\gamma\gamma$, γZ, ZZ, and WW) channels in the nonminimal CSTC (with scalar $\mu_{S,H}$ terms included) as functions of physical parameters of the model. The setup of parameters is the same as in Fig. 23.

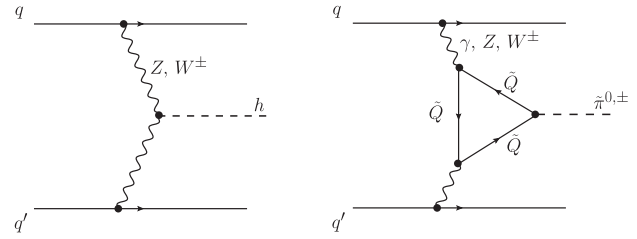

FIG. 25. Typical production channels of the Higgs boson at tree level (left) and technipion via a triangle technifermion loop (right) via gauge boson fusion in the quark-(anti)quark scattering.

of the produced state. An overall one-technipion production rate is expected to be strongly suppressed compared to the Higgs boson production rate, which along with extremely narrow technipion resonance makes it rather hard to measure experimentally but not impossible.

In Fig. 26, we show the one-technipion production cross sections via the VBF mechanism at the parton level for different incoming and outgoing quark q and (anti)quark q' states. Both parton-level and hadron-level cross sections at the LHC with $\sqrt{s} = 14$ TeV in the relevant kinematics and mass ranges along with corresponding Higgs boson cross sections in respective channels are presented [here and below, CTEQ5LO quark parton distribution functions (PDFs) [51] were used in calculations]. Only up and down quarks with at least one valence quark as well as contributions with maximal Cabibbo-Kobayashi-Maskawa mixing terms are included here. We have not applied any detector cuts or hadronization corrections here, which would be the next crucial step in phenomenological studies of the CSTC model. All the numerical estimates here are done for the first time in order to understand the potential of the suggested model. Even for a rather large technifermion-technipion coupling $g_{\mathrm{TC}} = 8$, we observe that the hadronic cross sections of the technipion production (middle panel) by about 2 orders of magnitude smaller than those for the Higgs boson (right panel) in the same mass range. This suppression will be even stronger for smaller g_{TC} coupling and does not depend on other CSTC model parameters. The respective production mechanism is thus one of the "golden" channels for technipion and, in general, new strongly coupled sector searches at the LHC in measurements with high statistics.

The discovery potential depends also on the subsequent decay modes and branching ratios of technipions. As was demonstrated above, the decay modes of the neutral technipion are similar to the vector-boson decay modes of the Higgs boson including $\gamma\gamma$, ZZ, and γZ channels; however, the $\tilde{\pi}^0 \to W^+W^-$ mode is forbidden by symmetry. In the range of relatively small $m_{\tilde{\pi}} \lesssim 200$ GeV, the strategy for searches of technipions will be similar to that in the Higgs boson searches. Moreover, for light technipions it turns out that the $\gamma\gamma$ signals from the Higgs boson and technipion can be comparable with each other due to a very small $\gamma\gamma$ branching ratio of the Higgs boson $\mathrm{BR}(h \to \gamma\gamma) \simeq 10^{-3}$, while corresponding technipion branching is relatively large $\mathrm{BR}(\tilde{\pi} \to \gamma\gamma) \simeq 0.5$–$1.0$ (see Fig. 22). The issue with detection of such light technipions in the $\gamma\gamma$ or γZ channels can arise, however, due to a very narrow technipion resonance, since in the mass range $\sim$150 GeV the total technipion decay width amounts to $\lesssim 0.1$ MeV (see Fig. 21). Such an extremely narrow resonance, in principle, can be missed in the Higgs-type searches at the LHC, and an additional investigation of this possibility is necessary. Also, the possibility of a relative proximity or even an overlap of the Higgs resonance and extremely narrow technipion resonance is not completely excluded and remains to be an interesting opportunity. Furthermore, a more elaborate analysis and the search for light technipions in the existing LHC data is required.

At last, heavier technipions $m_{\tilde{\pi}} \gtrsim 200$ GeV can be searched for in the $\gamma\gamma$, γZ, and ZZ decay channels which have comparable branchings. The dominant modes for the heavy Higgs boson searches are typically WW and ZZ ones with large branchings, whereas $\gamma\gamma$ and γZ branchings of

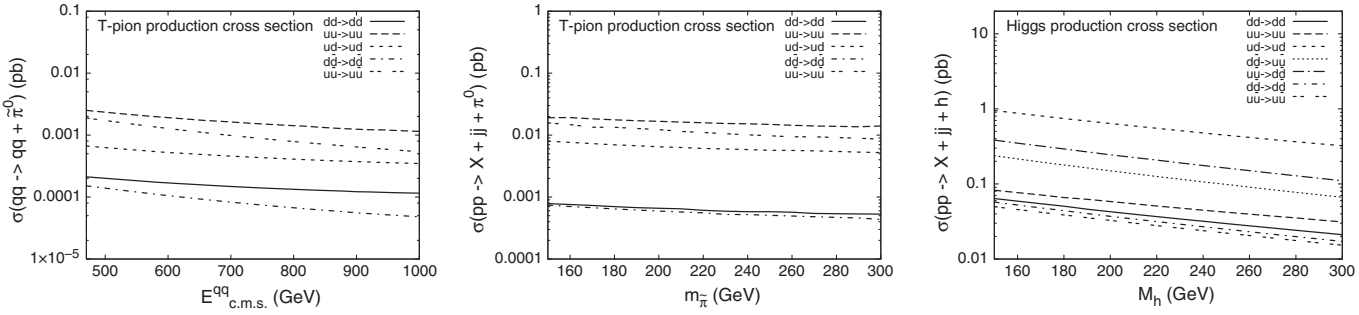

FIG. 26. The one-technipion (T-pion) production cross sections via the VBF mechanism at the parton level for different incoming and outgoing quark q and (anti)quark q' states as functions of qq' invariant mass, or c.m.s. energy $E^{qq}_{\mathrm{c.m.s.}} = \sqrt{\hat{s}}$ (left), corresponding total hadron level cross sections of one technipion production for given incoming qq' states in picobarns (before cuts) at the maximal LHC energy $\sqrt{s} = 14$ TeV as a function of the technipion mass $m_{\tilde{\pi}}$ (middle), and corresponding VBF hadronic cross sections of the Higgs boson as functions of its mass M_h shown for comparison. Here, $g_{\mathrm{TC}} = 8$ and $M_{\tilde{Q}} = 300$ GeV are fixed, and the results do not depend on other CSTC parameters. In calculations of the hadronic cross sections in this paper, we have used quark CTEQ5LO PDFs [51].

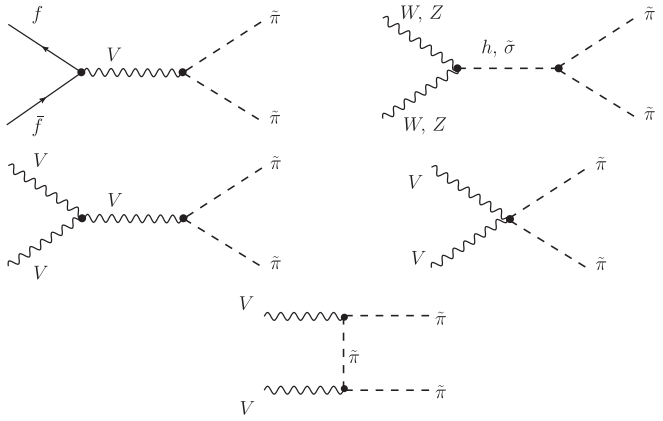

FIG. 27. Typical technipion production channels in the leading order, relevant for collider phenomenology. Here, $V = Z, W, \gamma$ in appropriate places. The ggh and $gg\tilde{\sigma}$ couplings are heavy quark loop-induced ones in the leading order.

the Higgs decay are practically zeroth. The only common channel for the technipion and Higgs boson in the high mass range is the ZZ one. However, having comparable branchings, the technipion production rate is strongly suppressed compared to that of the Higgs boson (see above). So, the current LHC statistics may not be enough for establishing significant constraints onto the CSTC model parameter space for the higher technipion masses, and further studies are certainly needed.

4. Technipion pair production

Typical leading-order (tree-level) processes of the $\tilde{\pi}$-pair production in $f\bar{f}$ and vector boson fusion at the LHC are shown in Fig. 27. Besides rather high $\tilde{\pi}\,\tilde{\pi}$ pair invariant mass $M_{\tilde{\pi}\tilde{\pi}} \gtrsim 300$ GeV, an additional suppression in VV and $f\bar{f}$ production channels appears due to rather weak couplings g and g^2 in $\tilde{\pi}\,\tilde{\pi}\,V$ and $\tilde{\pi}\,\tilde{\pi}\,VV$ vertices, respectively [cf. Eq. (2.26)], as well as due to a large off-resonant suppression in s-channel subprocesses with intermediate Higgs and gauge bosons, which are much lighter than $M_{\tilde{\pi}\tilde{\pi}}$.

Thus, one may naively assume that the largest contribution to the $\tilde{\pi}^+\tilde{\pi}^-$ and $\tilde{\pi}^0\tilde{\pi}^0$ production rates comes essentially from the intermediate technisigma resonance with the $\tilde{\pi}\,\tilde{\pi}\,\tilde{\sigma}$ coupling

$$g_{\tilde{\pi}\,\tilde{\pi}\,\tilde{\sigma}} = -g_{\rm TC} c_\theta \frac{M^2_{\tilde{\sigma}} - m^2_{\tilde{\pi}}}{2M_{\tilde{Q}}}, \tag{4.13}$$

which is not suppressed in the small mixing limit (for not very heavy technifermions). However, in the latter case, one encounters more sources of suppression. First, the production rate of the $\tilde{\sigma}$ itself in the SM-like channels is most likely to be suppressed by a small mixing angle, i.e., by the $s^2_\theta \ll 1$ factor in the cross section, compared to the Higgs boson production rate with $c^2_\theta \sim 1$ (see the previous section). Second, the $\tilde{\sigma}$ total decay width dominated by the technipion channel (in analogy to hadron physics) is typically large, of the order of a few hundred GeV, which means that there will be no resonant enhancement in the $\tilde{\pi}\,\tilde{\pi}$ production rate associated with the technisigma channel. Thus, overall rates of the tree-level $\tilde{\sigma}$ and $\tilde{\pi}\,\tilde{\pi}$ production are expected to be rather small, similarly to the loop-induced one-technipion rates calculated above. Moreover, in the small mixing or no $h\tilde{\sigma}$-mixing scenario, the only possible $\tilde{\sigma}$ production channel is through the gauge boson fusion through the technifermion and technipion triangles, since the $\tilde{Q}\,\tilde{Q}\,\tilde{\sigma}$ coupling (2.25) is finite:

$$g_{\tilde{Q}\,\tilde{Q}\,\tilde{\sigma}} = -g_{\rm TC} c_\theta, \tag{4.14}$$

and can be rather large due to the "fat" TC coupling $g_{\rm TC} > 1$. Besides the dominant technisigma decay mode, the $\tilde{\pi}\,\tilde{\pi}$ pair may also be produced at one-loop level via $\tilde{Q}$

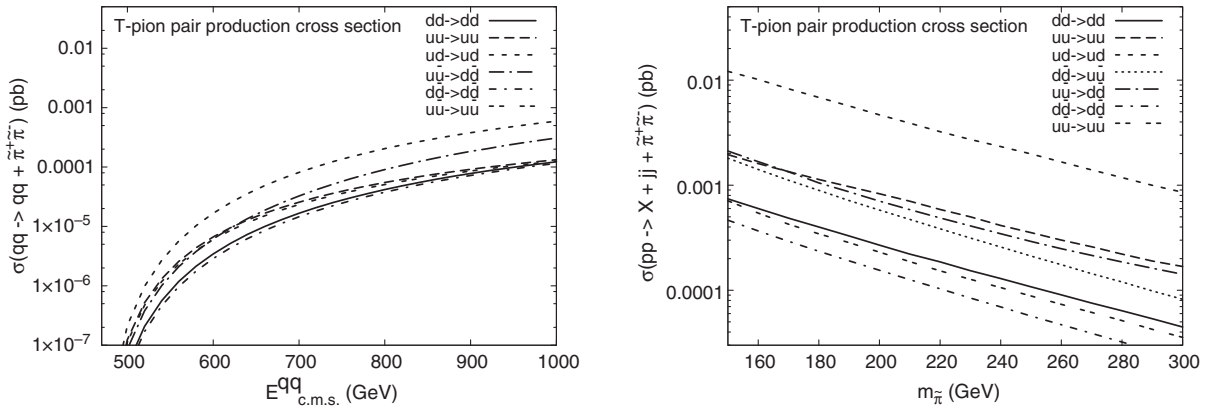

FIG. 28. The one-technipion (T-pion) pair production cross sections via the VBF mechanism at the parton level for different incoming and outgoing quark q and (anti)quark q' states as functions of qq' invariant mass, or c.m.s. energy $E^{qq}_{\rm c.m.s.} = \sqrt{\hat{s}}$ (left), corresponding total hadron level cross sections of the technipion pair production for given incoming qq' states in picobarns (before cuts) at the maximal LHC energy $\sqrt{s} = 14$ TeV as a function of the technipion mass $m_{\tilde{\pi}}$ (right). Here, $g_{\rm TC} = 8$, $c^2_\theta = 0.8$, $M_{\tilde{\sigma}} = 600$ GeV, and $M_{\tilde{Q}} = 300$ GeV are fixed.

box diagrams. These details of the lightest technihadron dynamics would make the search for new technipion and technisigma states rather challenging at the LHC, but not impossible.

For illustration, in Fig. 28, we present the $\tilde{\pi}^+\tilde{\pi}^-$ pair production cross sections at the parton level in the VBF mechanism as functions of the qq' center-of-mass (c.m.s.) energy for different initial and final quarks (left) and the corresponding hadron-level cross sections at the LHC ($\sqrt{s} = 14$ TeV) as functions of the technipion mass (right). The quark-antiquark fusion mechanism going via h or $\tilde{\sigma}$ resonance is assumed to be negligible in the forward and backward jets kinematics considered here and was not included in this calculation. Opposite to the one-technipion production cross sections shown in Fig. 26, the parton-level $\tilde{\pi}^+\tilde{\pi}^-$ pair production cross sections increase at higher qq' c.m.s. energies (or larger quark fractions x) and can reach the same magnitudes as the one-technipion cross sections at $E^{qq}_{\text{c.m.s.}} \gtrsim 700$ GeV. The hadronic $\tilde{\pi}^+\tilde{\pi}^-$ cross sections drop faster than corresponding one-technipion cross sections and have similar order-of-magnitude values for the light $\tilde{\pi}$ mass range. This means that both one- and two-technipion processes should be studied on the same footing. The latter, however, would be more difficult to identify experimentally due to a larger multiplicity of leptons and tiny widths of the technipions.

V. SUMMARY

In summary, in this work we have constructed and investigated in major detail the chiral-symmetric (vectorlike) technicolor scenario, according to which a new sector of technifermions in confinement interacts with the SM gauge bosons by means of vectorlike gauge couplings. Our analysis is based upon the gauged linear σ model with the initially global chiral-gauge $SU(2)_{\text{L}} \otimes SU(2)_{\text{R}}$ group broken down to the *local* LR-symmetric SM weak isospin symmetry $SU(2)_{L+R\equiv W}$ group in the technifermion sector.

The Higgs boson in this scenario is considered as a separate (fundamental or composite) scalar state and introduced in the same way as in the one-doublet SM. Nevertheless, we have shown that the electroweak symmetry breaking at the scale $M_{\text{EW}} \sim 100$ GeV can be initiated dynamically by the presence of the confined vectorlike technifermion sector; namely, it is triggered by the technifermion condensate at the techniconfinement scale, $\Lambda_{\text{TC}} \gtrsim M_{\text{EW}}$, together with the chiral symmetry breaking. This thus leads to the effective SM Higgs mechanism of dynamical electroweak symmetry breaking.

Remarkably, this model is well consistent with both EW precision constraints and, simultaneously, with the recent SM-like Higgs boson observations at the LHC in the small Higgs-technisigma mixing limit. At the same time, the model predicts the existence of extra new lightest technihadron states, namely, physical technipions $\tilde{\pi}$ and technisigma $\tilde{\sigma}$, at the LHC energy scales, giving rise to rich technicolor phenomenology at the LHC. Detection prospects for these new states have also been discussed, and the most phenomenologically important decay modes of $\tilde{\pi}$ and $\tilde{\sigma}$, as well as technipion production cross sections, were quantified over physically reasonable regions of parameter space.

In the absence of noticeable deviations from the SM predictions in the Higgs signal strengths, the suggested scenario is capable of explaining what triggers the SM Higgs mechanism, the nature of the Higgs VEV in the nearly conformal limit of the new strongly coupled dynamics. The proposed vectorlike technicolor scenario, in its simplest form considered here, does not attempt to resolve the naturalness problem of the SM, i.e., does not provide a mechanism protecting the Higgs boson mass itself from becoming arbitrarily large. Nevertheless, this minimal realization of the TC ideas preserving the effective Higgs mechanism of the SM opens up new prospects for more elaborate scenarios with extended chiral-gauge groups possibly predicting the light composite Higgs boson(s) with well-defined vectorlike ultraviolet completion, which is the subject of our further analysis. At last, as a specific prediction of this class of models, the lightest neutral heavy weakly interacting technibaryon state gives rise to a suitable dark matter candidate, making it an especially attractive opportunity for astrophysical new physics searches, and a corresponding analysis is planned for future studies.

ACKNOWLEDGMENTS

Stimulating discussions and helpful correspondence with Johan Bijnens, Gabriele Ferretti, Stefano Frixione, Christophe Grojean, Giuliano Panico, Sabir Ramazanov, Johan Rathsman, Slava Rychkov, Francesco Sannino, Torbjörn Sjöstrand, and Peter Skands are gratefully acknowledged. This work was supported in part by the Crafoord Foundation (Grant No. 20120520). R. P. is thankful to the CERN Theory Group for support and inspiring discussions during his visit at CERN. V. K. is especially grateful to the Lund THEP Group for support and hospitality during his visit at Lund University at the final stage of this work.

[1] ATLAS Collaboration, Phys. Lett. B **716**, 1 (2012); ATLAS Collaboration, Science **338**, 1576 (2012).
[2] CMS Collaboration, Phys. Lett. B **716**, 30 (2012); CMS Collaboration, Science **338**, 1569 (2012).
[3] T. Aaltonen *et al.* (CDF and D0 Collaborations), Phys. Rev. Lett. **109**, 071804 (2012).
[4] ATLAS Collaboration, Report Nos. ATLAS-CONF-2013-014 and ATLAS-CONF-2013-034; CMS Collaboration, Report Nos. CMS PAS-HIG-12-045 and CMS PAS-HIG-13-001.
[5] T. Aaltonen *et al.* (CDF and D0 Collaborations), Phys. Rev. D **88**, 052014 (2013).
[6] A. Falkowski, F. Riva, and A. Urbano, arXiv:1303.1812.
[7] J. Ellis and T. You, J. High Energy Phys. 06 (2013) 103.
[8] A. Djouadi and G. Moreau, arXiv:1303.6591.
[9] P. P. Giardino, K. Kannike, I. Masina, M. Raidal, and A. Strumia, arXiv:1303.3570.
[10] K. Cheung, J. S. Lee, and P.-Y. Tseng, J. High Energy Phys. 05 (2013) 134.
[11] S. Dittmaier *et al.* (LHC Higgs Cross Section Working Group Collaboration), arXiv:1101.0593; S. Dittmaier *et al.* (LHC Higgs Cross Section Working Group Collaboration), arXiv:1201.3084.
[12] S. Weinberg, Phys. Rev. D **13**, 974 (1976); L. Susskind, Phys. Rev. D **20**, 2619 (1979).
[13] S. Dimopoulos and L. Susskind, Nucl. Phys. **B155**, 237 (1979); E. Eichten and K. D. Lane, Phys. Lett. **90B**, 125 (1980).
[14] M. E. Peskin and T. Takeuchi, Phys. Rev. Lett. **65**, 964 (1990); Phys. Rev. D **46**, 381 (1992).
[15] C. T. Hill and E. H. Simmons, Phys. Rep. **381**, 235 (2003); **390**, 553(E) (2004).
[16] F. Sannino, Acta Phys. Pol. B **40**, 3533 (2009).
[17] T. W. Appelquist, D. Karabali, and L. C. R. Wijewardhana, Phys. Rev. Lett. **57**, 957 (1986).
[18] F. Sannino and K. Tuominen, Phys. Rev. D **71**, 051901 (2005).
[19] R. Foadi, M. T. Frandsen, T. A. Ryttov, and F. Sannino, Phys. Rev. D **76**, 055005 (2007).
[20] T. Alanne, S. Di Chiara, and K. Tuominen, arXiv:1303.3615.
[21] E. H. Simmons, Nucl. Phys. **B312**, 253 (1989).
[22] S. Samuel, Nucl. Phys. **B347**, 625 (1990).
[23] A. Kagan and S. Samuel, Phys. Lett. B **270**, 37 (1991).
[24] C. D. Carone, J. Erlich, and J. A. Tan, Phys. Rev. D **75**, 075005 (2007).
[25] C. D. Carone, Phys. Rev. D **86**, 055011 (2012).
[26] K. Agashe, R. Contino, and A. Pomarol, Nucl. Phys. **B719**, 165 (2005).
[27] J. Hirn and V. Sanz, Phys. Rev. Lett. **97**, 121803 (2006).
[28] D. K. Hong and H.-U. Yee, Phys. Rev. D **74**, 015011 (2006).
[29] R. S. Chivukula, arXiv:hep-ph/0011264.
[30] B. W. Lee and H. T. Nieh, Phys. Rev. **166**, 1507 (1968).
[31] S. Gasiorowicz and D. Geffen, Rev. Mod. Phys. **41**, 531 (1969); P. Ko and S. Rudaz, Phys. Rev. D **50**, 6877 (1994); M. Urban, M. Buballa, and J. Wambach, Nucl. Phys. **A697**, 338 (2002).
[32] B. D. Serot and J. D. Walecka, Acta Phys. Pol. B **21**, 655 (1992).
[33] Y. Nambu and G. Jona-Lasinio, Phys. Rev. **122**, 345 (1961); D. Ebert and M. K. Volkov, Z. Phys. C **16**, 205 (1983); M. K. Volkov, Ann. Phys. (N.Y.) **157**, 282 (1984).
[34] U. Vogl and W. Weise, Prog. Part. Nucl. Phys. **27**, 195 (1991).
[35] W. A. Bardeen, C. N. Leung, and S. T. Love, Phys. Rev. Lett. **56**, 1230 (1986); C. N. Leung, S. T. Love, and W. A. Bardeen, Nucl. Phys. **B273**, 649 (1986); M. Harada, Y. Kikukawa, T. Kugo, and H. Nakano, Prog. Theor. Phys. **92**, 1161 (1994).
[36] V. A. Miransky, *Dynamical Symmetry Breaking in Quantum Field Theories* (World-Scientific, Singapore, 1993).
[37] T. Eguchi, Phys. Rev. D **14**, 2755 (1976); K. Kikkawa, Prog. Theor. Phys. **56**, 947 (1976); M. K. Volkov, Fiz. Elem. Chastits At. Yadra **17**, 433 (1986) [Sov. J. Part. Nucl. **17**, 186 (1986)].
[38] M. Green and J. Schwarz, Phys. Lett. **149B**, 117 (1984).
[39] B. D. Serot, Phys. Lett. **86B**, 146 (1979); **87B**, 172 (1979).
[40] U.-G. Meibner, Phys. Rep. **161**, 214 (1988); B. D. Serot and J. D. Walecka, Int. J. Mod. Phys. E **06**, 515 (1997).
[41] M. A. Shifman, A. I. Vainshtein, and V. I. Zakharov, Nucl. Phys. **B147**, 385 (1979).
[42] D. V. Shirkov and I. L. Solovtsov, Phys. Rev. Lett. **79**, 1209 (1997).
[43] I. Maksymyk, C. P. Burgess, and D. London, Phys. Rev. D **50**, 529 (1994).
[44] C. P. Burgess, S. Godfrey, H. Konig, D. London, and I. Maksymyk, Phys. Lett. B **326**, 276 (1994).
[45] J. Beringer *et al.* (Particle Data Group), Phys. Rev. D **86**, 010001 (2012).
[46] R. Barbieri, A. Pomarol, R. Rattazzi, and A. Strumia, Nucl. Phys. **B703**, 127 (2004).
[47] B. A. Kniehl, Phys. Rep. **240**, 211 (1994).
[48] G. Passarino and M. J. G. Veltman, Nucl. Phys. **B160**, 151 (1979).
[49] H. S. Fukano and F. Sannino, Int. J. Mod. Phys. A **25**, 3911 (2010).
[50] V. I. Kuksa, Phys. Lett. B **633**, 545 (2006); **664**, 315(E) (2008); Int. J. Mod. Phys. A **23**, 4509 (2008); **24**, 4221(E) (2009).
[51] H. L. Lai, J. Huston, S. Kuhlmann, J. Morfin, F. Olness, J. F. Owens, J. Pumplin, and W. K. Tung (CTEQ Collaboration), Eur. Phys. J. C **12**, 375 (2000).